Int J Earth Sci (Geol Rundsch) (2014) 103:1889–1916
DOI 10.1007/s00531-014-1010-0

REVIEW ARTICLE

Marine cold seeps and their manifestations: geological control, biogeochemical criteria and environmental conditions

Erwin Suess

Received: 24 June 2013 / Accepted: 24 February 2014 / Published online: 26 March 2014

Abstract Characteristics of cold seeps at different geologic settings are the subject of this review primarily based on results of the Research Consortium SFB 574. Criteria are drawn from examples on the erosive convergent margin off Costa Rica, the accretionary margin off Chile supplemented by examples from the transform margin of the Golf of Cadiz and the convergent Hikurangi margin off New Zealand. Others are from well-studied passive margins of the Black Sea, the Golf of Mexico, the eastern Mediterranean Sea and the South China Sea. Seeps at all settings transport water and dissolved compounds to the ocean through the seafloor by different forcing mechanism and from different depths of the submerged geosphere (10s of meters to 10s of km). The compounds sustain oasis-type ecosystems by providing bioactive reductants sulfide, methane and hydrogen. Hereby, the interaction between fluid composition, flux rates and biota results in a diagnostic hydrocarbon–metazoan–microbe–carbonate association; currently, well over 100 active sites are known. The single most important reaction is microbially mediated anaerobic oxidation of methane with secondary reactions involving S-biogeochemistry and carbonate mineral precipitation. Seep fluids and their seafloor manifestations provide clues as to source depth, fluid–sediment/rock interaction during ascent, lifetime and cyclicity of seepage events but less so on the magnitude of return flow. At erosive margins, Cl-depleted and B-enriched fluids from clay dehydration provide criteria for source depth and temperature. The upward material flow generates mud volcanoes at the seafloor above the projected location of dehydration at depth. At accretionary margins, fluids are derived from more shallow depths by compaction of sediments as they ride on the incoming oceanic plate; they are emitted through thrust faults. At highly sedimented margins, organic-rich and evaporite-containing strata (when present) determine the final fluid composition, by emitting characteristically gas hydrate-derived methane, brine-associated non-methane hydrocarbons or leached elements and their isotopes (Li, δ^7Li, B, Ba) from host sediments. Smectite–illite transformation and associated Cl-depletion from release of interlayer water is a pervasive process at these margins. Rare earth element pattern in conjunction with redox-sensitive metals retained in seep carbonates indicate whether or not they precipitated in contact with oxic bottom water or suboxic fluids; clear environmental characterization, though, currently remains inconclusive. More deeply sourced fluids as in transform margins may be characterized by their $^{87}Sr/^{86}Sr$ ratios from interaction with oceanic crustal rocks below. Quantification of flow and reliable estimates of total volatile output from fore-arcs remain a challenge to seep research, as does understanding the role of geologically derived methane in the global methane cycle.

Keywords Seep carbonates · Fore-arc fluids · Global seeps · Biota–carbonate association · Active margin fluids · Passive margin seeps

E. Suess (✉)
GEOMAR Helmholtz Centre for Ocean Research Kiel,
Wischhofstr. 1-3, 24148 Kiel, Germany
e-mail: esuess@geomar.de

E. Suess
College of Earth, Ocean, and Atmospheric Sciences,
Oregon State University, Corvallis, OR 97331-5503, USA

Introduction

Transfer from the geosphere to the exosphere (biosphere, hydrosphere, atmosphere) is a fundamental process of the Earth's material recycling. Many sub-cycles and pathways

are active on different timescales and moving different magnitudes of material. Plate boundaries, volcanic arcs and continental margins are the geologic settings that largely determine this transfer process. A unique pathway of material transfer is by seepage of volatile elements and compounds from marine cold seeps and from mud volcanoes when lithic material and fluids are transported together. Geologic settings, biogeochemical reactions and biologic activities are uniquely interconnected to generate the seep products. These come in many shapes and sizes from which environmental conditions, the history and extent of fluid–sediment reactions may be derived. The magnitude of recycled material through seeps is poorly known despite the easily recognizable and mappable seep manifestations. This issue remains a challenge to seep research at subduction zone settings, as does the role of the geologically derived methane in the global carbon cycle (Boetius and Wenzhöfer 2013).

Seeps sustain unique oasis-type ecosystems at the seafloor, here referred to as *the hydrocarbon–metazoan–microbe–carbonate association*. They occur globally along active margins driven by plate convergence and along passive margins by sediment loading and by differential compaction related to vertical tectonics (Fig. 1). Seeps characteristically flow more slowly than hydrothermal vents and are usually at ambient seafloor temperature, as the terminology implies. More vigorously flowing seeps may show elevated temperatures as may active mud volcanoes. Long-standing objectives of seep studies have been the quantification of water and carbon transfer, characterization of source depth, and the role of seep transport in global element recycling. These were part of the overarching objective of the Research Consortium SFB 574 by the German Science Foundation entitled: "Volatiles and Fluids in Subduction Zones" (Wallmann 2001; Jarrard 2003; Rüpke et al. 2004; Scholl and von Huene 2007; Freundt et al. 2014). Global geologic settings provide an enormous range of depth levels in the Earth's crust for fluid generation. Seeps range for example from effluents of shallow groundwater aquifers, underlying shelves of a few 10s of meters, to waters expelled through oceanic fore-arcs generated 10s of km below from underlying tectonic plates. On passive margins, the nature and thickness of the accumulating sediment package determine seepage and products variously consisting of mud volcanoes, pockmarks, brine lakes but dominantly of authigenic carbonates. They form above rapidly accumulating, organic-rich sediments, deltaic aprons, hydrocarbon reservoirs or buried evaporites. Return

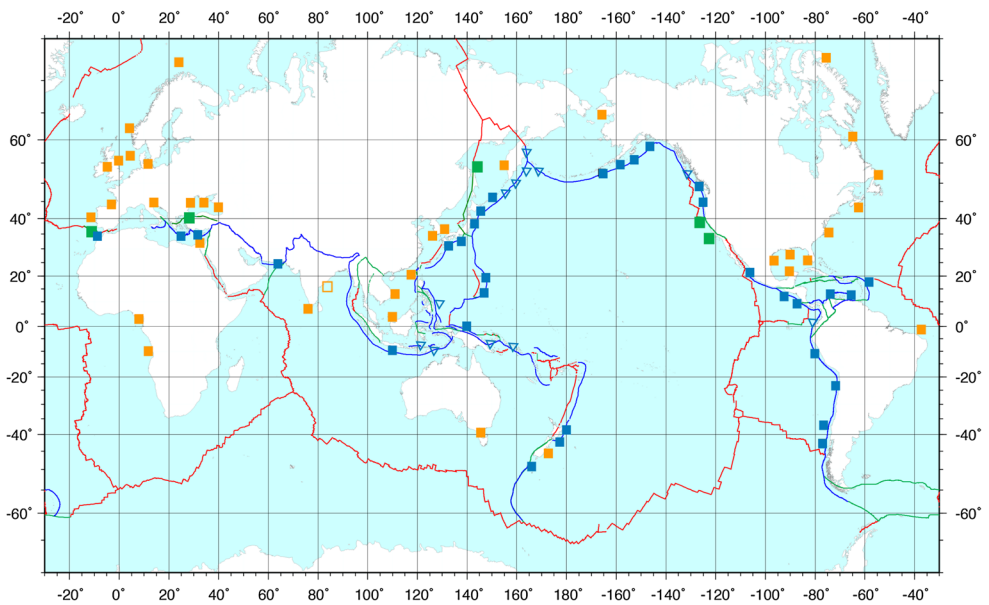

Fig. 1 Global cold seeps. Seep locations with hydrocarbon–metazoan–microbe–carbonate characteristics; active margins sites (*blue*), passive margin sites incl. groundwater seeps (*orange*); sites at transform margins (*green*). Distribution based on first seep location maps by Campbell (2006) with site references. New sites are from Jeong et al. (2004), Loncke et al. (2004), Olu-Le Roy et al. (2004, 2007), Judd et al. (2007), Mastarlerz et al. (2007), Hovland (2007), Han et al. (2008), Sahling et al. (2008), Geli et al. (2008), Hilario and Cunha (2008), Sellanes et al. (2008), Pierre and Fouquet (2007), Niemann et al. (2009), Bayon et al. (2007), Iglesias et al. (2010), Gracia et al. (2010); dead seep clam site off India (*open square*) from Collett et al. (2008). Sites based on dredged tube worms (*open triangles*), mostly at deep-sea trenches, are from Ivanov (1963) prior to recognition that seep communities at plate boundaries are sites of hydrocarbon seepage. Updates of new site locations and descriptions are in: Garcia-Gil and Judd (2007), Bohrmann and Jørgensen (2010), De Batist and Khlystov (2012), Pierre et al. (2014). Maps of global distributions of seep biota can be found in: Krylova and Sahling (2010), German et al. (2011)

flow at active margins is generally more deeply sourced than at passive margins. Characterization cannot be based on margin tectonics alone, however, because reactions with host materials overprint the seep fluid composition during upward flow and the formation of the resulting seep products.

The seep characteristics at different geologic settings are the subject of this review. New knowledge gained is highlighted as it relates to the lifespan of seeps, source depth of fluids, impact of host sediment and characterization of the biogeochemical environment. Speculation on future research concludes the contribution; e.g., reconciling and improving estimates of volatile outflows from fore-arcs, comparing approaches best taken to advance understanding of ancient seeps, and continuing to develop proxies for environmental characterization. The goal is to present a worldwide view of seep studies as currently documented in several special issues (Zhang and Lanoil 2004; Bohrmann and Jørgensen 2010; Roberts and Boland 2010; de Batist and Khlystov 2012; Matsumoto et al. 2011; Pierre et al. 2014 in prep). Whereas most of these report on isolated sites or selected examples of methane seepage, however, the Hikurangi margin project off New Zealand (Greinert et al. 2010) is remarkable as an interdisciplinary approach that brings advanced tools of seep research to a single area. To a degree, this project appears to be a more detailed blue print of the subduction zone input/output objectives at fore-arcs initially addressed by the SFB 574 consortium. The Hikurangi results are compiled from seismic studies, water column characterization, direct ROV observations, seep biology and authigenic carbonates and are here considered—whenever appropriate—together with the SFB 574 results from offshore Costa Rica and southern Chile. In that way, this review provides a reference frame, in some instances going back to and crediting original publications, about the current state-of-the-art of seep research with emphasis on subduction zone settings.

Seeps at active plate margins

Oceanic plate and continental plate convergence

By far, the most frequent and best-studied seafloor seeps worldwide occur at the convergence between oceanic and continental plates and extend from upper continental slopes to deep trenches. Indeed, it was research at global convergent margins that first revealed the uniqueness of seeps and their products resulting from large-scale fluid expulsion by dewatering of sediments (Suess et al. 1985; Kulm et al. 1986; LePichon et al. 1987). The dewatering occurs in response to lateral compression from plate movement. Sediment-laden oceanic plates move underneath less dense continental plates. Sediments are either scraped off and accreted onto the edge of the overriding plate or are bypassed at its base to become subducted or underplated. Off-scraping and by-passing lead to two types of subduction margins—accretionary and erosive (also referred to as non-accretionary)—typically along the global deep-sea trench system generating seep fluids and products from different depths (Scholl and von Huene 2007; Wannamaker et al. 2009; Moore et al. 2011).

Accretionary margins consist of a series of ridges oriented parallel to the trench axis made up largely of compressed, folded and faulted turbidite or trench-fill deposits (Fig. 2). In landward troughs between the ridges, the fore-arc basins, thick hemi-pelagic sediments are deposited on the slopes. The ridges as well as the basins are the source of seep fluids. Over extended periods of accretion the ridges are increasingly deformed into landward-verging structural packages separated by thrust faults. These packages constitute the accretionary prism. Farther landward they abut the continental framework rock (backstop) that comprises the upper continental plate. The surface of the framework rock continues to accumulate unconformably seaward prograding slope sediments. Where the subduction angle is shallow as off southern Chile, Cascadia or Japan, convergence causes splay faults to develop in the framework rock that drain the upper plate (Moore et al. 2007; Torres et al. 2004, 2009; Geersen et al. 2011; Scholz et al. 2013). Composition and properties of the upper plate framework rock are of vital importance to the behavior of the entire subduction zone, including fluid generation and transport, whether of the accretionary or erosive type.

Where the subduction angle is steep or the surface of the descending oceanic plate is “rough” as off Costa Rica, the base of the upper plate is being eroded and/or experiences underplating of sediments that escaped being scraped off the descending plate thus leading to erosive or non-accretionary margins. According to Scholl and von Huene (2007), 75 % of the global subduction zones are non-accretionary. The underplated sediments constitute the subduction channel, an increasingly recognized site for deep-seated reactions between trapped seawater-derived fluids and seawater-altered oceanic host rocks (van der Straaten et al. 2012). At erosive margins, small accretionary prisms develop near the trench, but most sediments are carried downward with the oceanic plate, thereby removing material from or adding to the underside of the overriding plate. As a consequence, the margin subsides, fractures, and eventually the plate’s edge is destroyed (Fig. 3). The destructive action at the plate’s edge is particularly severe when volcanic seamounts are subducted. These elevated basaltic features, riding on the oceanic crust, arrive at the trench and plough into the continental margin leaving scars and scarps (Ranero and von Huene 2000; Barnes et al.

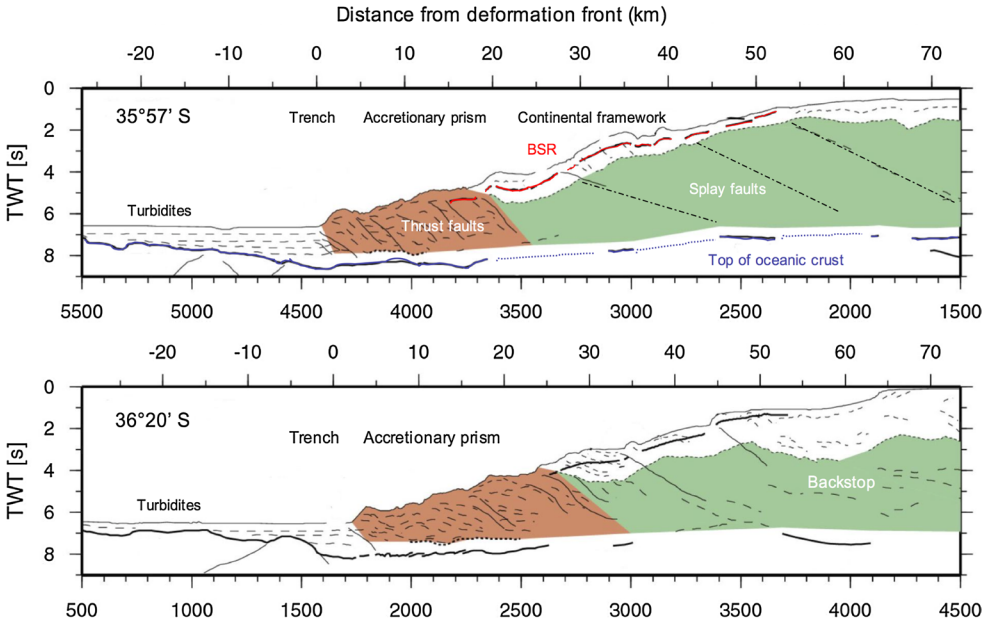

Fig. 2 Accretionary margin. Convergent margin off southern Chile with trench turbidites, accretionary prism, continental framework rock (backstop), and hemi-pelagic sediment cover. Subduction channel between top of oceanic curst and accretionary and continental framework rocks. Fluid escape features are thrust faults separating accretionary ridges, sometimes with basins between them, and splay faults cutting through the continental framework rocks. Hemi-pelagic sediment cover with well-developed bottom simulating reflector (BSR). Distance in (km) landward and seaward from the deformation front (deep-sea trench); seismic velocity TWT = two-way travel time (s) indicating sediment and rock thicknesses; based on Geersen et al. (2011), Scholz et al. (2013), Reston (pers. com)

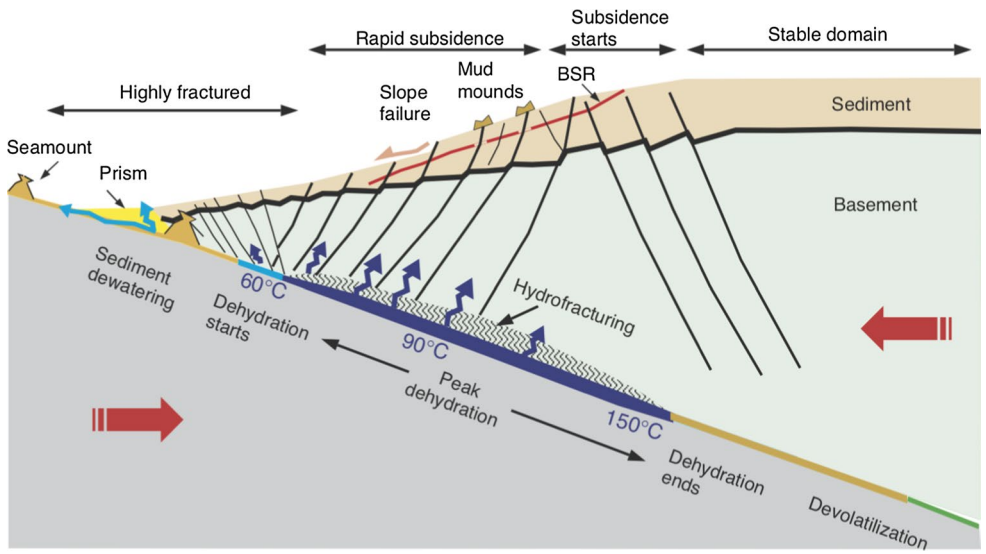

Fig. 3 Erosive margin. Convergent margin off Costa Rica with small accretionary prisms, highly fractured edge of continental plate, region of pronounced subsidence due to removal (erosion) of material from plate underside, and stable continental framework rock; all features covered by seaward prograding hemi-pelagic sediments with well-developed bottom simulating reflector (BSR). Fluid escape features on *lower-middle* slope are mud volcanoes situated above temperature–pressure regime of mineral dehydration from top of down-going plate. Fluids and muds are forced upward through deep-reaching fractures. Subducted volcanic seamounts contribute to destruction of overriding plate edge leaving scars, scarps, faults and bulges that facilitate fluid escape; modified from Ranero and von Huene (2000), Ranero et al. (2008)

2010). Ensuing slope failures, faulting and bulging of the sediment strata greatly facilitate fluid escape and seep formation (Mau et al. 2012). Subducted seamounts also pose a major earthquake hazard. It is near the front where seeps initially form. Farther under the overriding plate, increasing temperatures and higher pressures release mineral-bound

water by dehydration, forcing large amounts of fluids upward through splay faults. Fluids mixed with mud form mud volcanoes and seeps, preferentially aligned above subsurface isotherms consistent with clay mineral dehydration (Ranero et al. 2008; Sahling et al. 2008; Buerk et al. 2010).

Recent drilling into the overriding plate off Costa Rica suggests that the framework rocks, initially thought to be oceanic lithologies derived from the offshore extension of the Carribean Large Igneous Province (Vannucchi et al. 2006), consist to a significant degree of cemented fore-arc basin sediments (IODP Prelm. Rept., 344; 2013). These lithologies may impart characteristics to the fluids and solids that are transported upward presumably along splay faults imaged as high-amplitude, landward-dipping reflectors that cut through the fore-arc and appear to be offset at the unconformity with the overlying slope sediments (Ranero et al. 2008). These faults drain the deeper part of the margin and focus fluids and sediments to escape and build up the mud volcanoes aligned along the margin.

A significant input of water and volatile elements is through hydration (serpentinization) of the oceanic plate during subduction. Although this had been suspected for some time (Peacock 2001) but not until it was shown that bend-faulting facilitates deep penetration of seawater into the oceanic lithosphere which significantly alters seismic velocities, did it become possible to quantify the degree of serpentinization and hence water input (Ranero et al. 2003; Rüpke et al. 2004; Ivandic et al. 2010). Bend-faulting results from flexure of the oceanic lithosphere causing fractures that reach as deep as the upper mantle. Bend faulting is well-developed off NW Costa Rica and Nicaragua where the old and rigid portion of the Cocos plate that formed at the fast-spreading East Pacific Rise is subducted underneath the Caribbean Plate. Farther southeast off central Costa Rica (Nicoya Peninsula) the slightly younger portion of the Cocos Plate that formed at the Cocos Nazca spreading center is also subject to bend faulting and water intake but less intensive (Fig. 4). Seismic velocity changes of the altered lithosphere indicate that the water intake is substantial and off Nicaragua about 2.5 times lager than off central Costa Rica (van Avendonk et al. 2011).

Other evidence for water intake comes from electrical resistivities derived from magnetotelluric imaging of the margin. Worzewski et al. (2010) showed several domains of increased conductivity indicating the presence of fluids. Two of these coincide with the decrease in seismic velocity and might be of relevance to seep fluids. The first is a conductivity anomaly along the incoming plate related to seawater intake through bend faults and release of water through pores and cracks. Hereby, the release of water is not evident in conductivity changes. The second anomaly occurs at the plate interface and documents increased conductivity presumably related to dehydration of sediments.

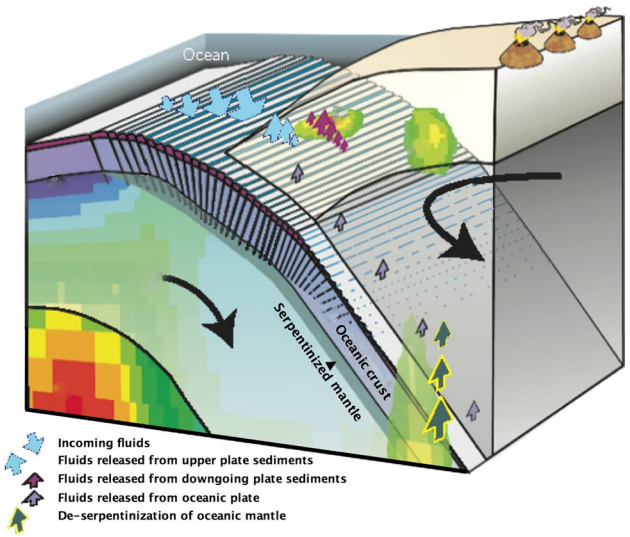

Fig. 4 Serpentinized margin. Prominent bend faulting of incoming Cocos Plate off Nicaragua and NW Costa Rica facilitates deep penetration of seawater into the oceanic lithosphere causing serpentinization of mantle rocks. Water uptake significantly alters seismic velocities and electrical properties. These anomaliesd indicate several regimes with fluids emitted in the fore-arc: from upper plate sediments (*light blue arrows*); from dehydration of down-going plate sediments (*purple arrows*). Deeper anomalies (>30 and 100 km) indicate fluids derived from heating of the mantle wedge and de-serpentinization of the oceanic mantle; these are not emitted in the fore-arc; modified from Worzewski et al. (2010) with information from Ivandic et al. (2010)

Deeper anomalies up to 30 km and 100 km, the authors relate to fluid accumulation derived from heating of the mantle wedge and de-serpentinization of the oceanic mantle, respectively. These anomalies cannot be imaged by seismic nor do they contribute to fore-arc seeps.

Oceanic plate and oceanic plate convergence

Emission of deep-sourced fluids containing abiotic methane plus traces of non-methane hydrocarbons and hydrogen is observed at the convergence of two oceanic plates in the Mariana fore-arc (Fryer et al. 1995; Mottl et al. 2004). The down-going plate contains little sediment leaving its top to undergo hydration by reacting with seawater at shallow depth to form serpentinite. But as temperature and pressure increase at greater depth, the top of the down-going plate is dehydrated again (de-serpentinization). This may take place as deep as 30 km below the seafloor. The liberated fluids ascend and compound hydration of the overlying oceanic plate. The hydration reactions form serpentine from olivine- and pyroxene-rich crustal rocks. The alteration products are carried upward, along with the excess of fluids, and exit as seeps forming serpentinite mud volcanoes. The abiotic production of non-methane hydrocarbons (C_2H_6, C_3H_8, n-C_4H_{10}, i-C_4H_{10} and others) receives much

attention for its far-reaching implications not the least to the origin of life (Prokurowski et al. 2008; Koleshnikov et al. 2009; National Geographic Magazine, June 2013). The area of the southern Mariana Arc including the Challenger Deep and Sirena Deep in the trench, the serpentine mounds and arc volcanoes have been declared in 2009 the Marianas Trench Marine National Monument, administered by the U.S. National Fish and Wildlife Service.

Understanding hydration reactions has been advanced by investigating slow-spreading oceanic ridge segments at which ultramafic rocks are within reach of penetrating seawater and by experimental work of rock–water interactions (Palandri and Reed 2004). On the Mid-Atlantic Ridge, hydrothermal vent fluids from serpentinized oceanic crust form aragonite and calcite chimneys (Ludwig et al. 2006). However, none have been reported so far from serpentinized portions of the oceanic plate entering the subduction zone.

Transform plate boundaries

Transform boundaries generate prolific cold seeps where they crosscut thick sedimentary sequences providing fluid pathways for expulsion along the fault planes. The first cold seep biota and barite precipitates were discovered at the San Clemente transform but mistaken for manifestations at hydrothermal vents of oceanic spreading centers (Lonsdale 1979) and later correctly identified as cold seep products (Torres et al. 2002). At transform boundaries, two plates slide past each other with only horizontal movement between them either threatening earthquakes if they are locked or facilitating reactions during slow creep if fluids are present. Seeps at transform boundaries have not previously been considered in their own right, but since plate margins are involved, the fault planes reach to great depths and hence a deep-source signal might be expected. Transform faults at continental margins pose earthquake hazards; e.g., San Andreas Fault, Anatolian Fault system, Sakhalin Transform fault, the Queen Charlotte Fault and the Gulf of Cadiz; hence research on gas and fluid seepage and their products—largely in form of authigenic carbonates and methane-rich fluids—has recently focused on such tectonic settings (Shakirov et al. 2004; Geli et al. 2008; Carpenter et al. 2011; Gutscher et al. 2012; Halliday et al. 2008; Barrie et al. 2013).

Seeps at passive continental margins

On passive margins, the variety of geologic settings, the mechanisms of fluid expulsion and the worldwide occurrence of cold seeps are immense (Fig. 5). Pockmarks on shelves and slopes are expressions of seeps fed from submerged aquifers, from overpressured formations containing hydrocarbons and brines, or from rapidly deposited accumulations of water-rich sediments. Hydrocarbon seeps have long guided offshore exploration for oil and gas deposits (Judd and Hovland 2007).

Groundwater seepage from sub-seafloor extensions of aquifers has been known since the early days of seafarers. Discharge of sulfide-rich hypersaline water feeding ventlike biological communities was first reported off the

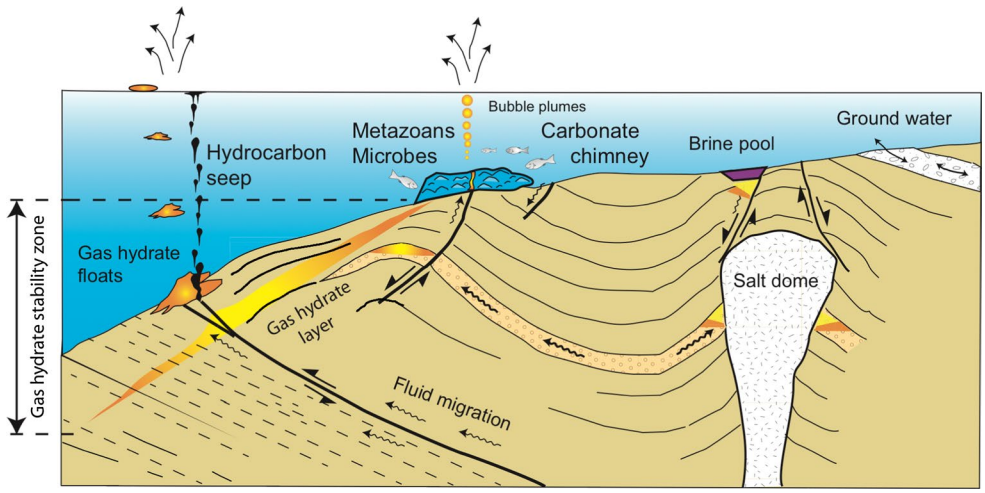

Fig. 5 Passive margin. Geologic settings and the mechanisms of fluid expulsion generate an enormous variety cold seeps ranging from pockmarks on shelves and slopes caused by outflow from submerged aquifers, overpressured formations containing hydrocarbons and brines and rapidly sedimented water-rich sediments in deltas or drift deposits. Carbonate chimneys, asphalt seeps, methane hydrate mounds, seep fauna and methane plumes in the water column are the ubiquitous manifestations. Methane hydrate rafts-infrequently observed-transfer methane directly from the seafloor to the atmosphere (Pape et al. 2011); modified from Suess and Linke (2006) based on Moore (1999)

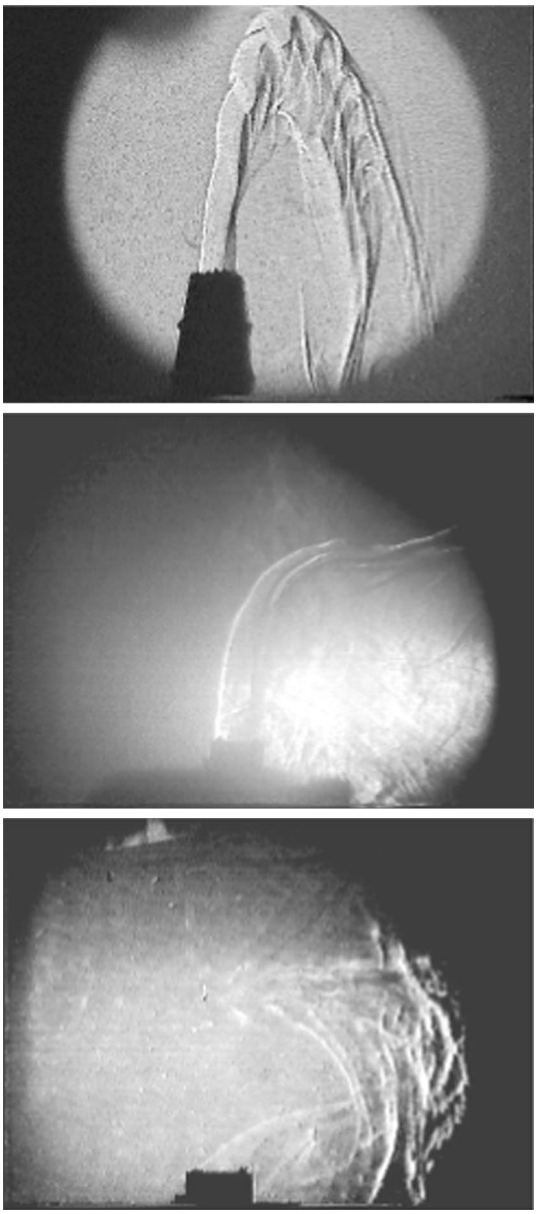

Fig. 6 Seep flow imaged. Visualizating fluid flow from cold seeps based on optical "schlieren" technique that is sensitive to small changes in refractive index from temperature and salinity differences. (*top*) Flume experiment with saline fluid ejected through an opening; diameter of image = 5 cm; (*middle*) channeled fresh water seep at the seafloor (water depth 18 m); (*bottom*) weakly channeled seep fluids at Hydrate Ridge (water 780 m) laterally displaced by bottom current; modified from Suess and Linke (2006) based on Karpen et al. (2004)

Florida Escarpment (Paull et al. 1984). Today groundwater seepage carries pesticides, herbicides and fertilizer residues into shelf waters off coastal areas. Pumping for drinking water depletes groundwater reservoirs and allows seawater to enter or high tidal ranges force it back into the aquifers. The result is widespread salt invasion of groundwater in coastal areas and other problems regarding global groundwater reservoirs (Gallardo and Marui 2006). Submarine groundwater discharge may be estimated by ^{222}Rn measurements (Peterson et al. 2008).

The driving mechanisms for fluid expulsion at passive margins are: loading by sediment, differential compaction, overpressure and facies changes. Hence, rapidly accumulating water-rich sediments generate seeps and mud volcanoes in deltas, in deep-sea fans and along passive margins as well as in marginal seas. In short, any changes involving different permeabilities of fluid-rich strata, such as ash layers, turbidites, sands and silts (deltas), drift sediments, even buried reefs when intersected by faults, open up pathways for fluid escape. Other driving forces for seepage are free gas movement (buoyancy), hydrological and tidal pumping and thermally driven fluid and gas circulation. Several methods have been used to image fluid flow (Fig. 6; Karpen et al. 2004) and directly measure expulsion rates at seep sites of passive and active margins. Reliability largely depends on the flow rate. Slow rates are estimated by modeling pore water profiles (Hensen et al. 2004; Karaca et al. 2012; many others) and are suited for a method employed by Tryon et al. (2001). High rates are suitable for quantification by flux meters deployed by benthic landers (Linke et al. 2005).

Common seep characteristics at active and passive margins

The type of fluids expelled back into the ocean at accretionary, erosive and transform margins or at passive margins—whether from deep or shallow sources—depends on the thickness and provenance of the sediment column, the rate of sedimentation, the age and cooling history of the subducted plate and the morphology of the moving or stationary plates. Organic-rich and evaporite-containing strata represent end-members of the above spectrum in determining the final seep fluid composition and their recognizable products at the seafloor.

Sedimented margins

The subduction of sedimented oceanic plates provides the first-order input of volatile elements to the Earth's material recycling (Jarrard 2003; Scholl and von Huene 2007; Freundt et al. 2014). In terms of thickness of the sediment package and its provenance, the sedimented convergent margins are not much different from passive margin. Hence, reactions between fluids and components in hemipelagic passive margin sediments, inside the accretionary prisms, with the backstop rocks and the sediment blanket draped over the margin from shelf depths to the trench, determine the seep fluids, their products and return pathways to the seafloor.

Fluids expelled through seeps at sedimented margins contain the remineralized nutrients (silica, phosphate, ammonia and alkalinity) and hydrogen sulfide, as well as dissolved and free methane from microbial degradation of sedimentary organic matter. Thick sediments often are deposited along continental margins associated with coastal upwelling or otherwise high primary productivity in response to nutrient loading from nearby continents. Such sediments are rich in organic matter, biogenic silica; they accumulate rapidly and thus greatly favor sulfate reduction and methanogenesis of the microbially mediated early diagenetic reaction sequence.

Most sedimented margins generate enough biogenic methane that, when moving upward, exits as dissolved or free gas directly into the bottom water, or alternatively when reaching the methane hydrate zone, is retained in layers of gas hydrate. Whereas free gas ascends through seismically anomalous conduits (acoustic blanket zones; gas chimneys) and forms acoustically detectable plumes in the water column, gas hydrate layers are detected seismically as bottom simulating reflectors (Tinivella and Lodolo 2000). Among the products of seeps emanating from the seafloor the association of biota and authigenic carbonates is by far the most widely encountered "archive" from which source depths, environmental conditions and tectonic settings may be inferred (Liebetrau et al. 2014).

The hydrocarbon–metazoan–microbe–carbonate association

Fluid flow, bioirrigation and bubble-induced mixing at seeps (Sahling et al. 2003; Haeckel et al. 2007) drive the interaction between anaerobic oxidation of methane (AOM), communities of macrobiota and formation of carbonates and sulfides (Fig. 7). Methane, either from subsurface gas hydrate, from ascending bubbles or as dissolved gas, supplies the AOM-consortia that aggregate at different sub-seafloor depths (Reaction 1). The consortia generate hydrogen sulfide that rises and is oxidized either in microbial mats at the surface or by symbionts within the macrofauna, using oxygen or nitrate (Reactions 2a and 2b). When mobile iron is present, the hydrogen sulfide may be fixed as iron sulfides (no such reaction is shown in Fig. 7 but discussed at length by Boetius and Wenzhöfer 2013). Bivalves pump oxygen downward, whereas tubeworms (not shown in Fig. 7) extract hydrogen sulfide through their roots (Freytag et al. 2001). As a consequence of the AOM-activity, calcium carbonate phases precipitate (Reaction 3). Earlier views favored accidental reaction from the byproduct of AOM, now it is thought plausible that the microbial community may actively promote precipitation even of selected mineral phases (Haas et al. 2010; Krause et al. 2012).

Anaerobic oxidation of methane

Subsurface gas hydrates and ascending free methane at seeps provide the C-reservoir for the AOM-consortia that consume interstitial sulfate (Boetius et al. 2000; Orphan et al. 2001; Milucka et al. 2012). The steep gradient of sulfate within the near-surface sediments is a reliable indicator for rapid upward flow of methane-rich seep fluids (Knittel et al. 2003). The subsurface depth of the sulfate–methane interface has become a standard indicator for mapping seep locations and exploring for gas hydrates. Methane usually originates from fermentative decomposition of organic matter or is produced by bacterial CO_2 reduction. In some settings, gas hydrate forms from thermogenic methane that migrates from deeper hydrocarbon reservoirs (Sassen et al. 2004; MacDonald et al. 2004). The sources can readily be distinguished by stable C- and D/H-isotopes of CH_4 (Whiticar 1999).

Gas hydrates form from methane-supersaturated pore fluids at elevated pressure (>60 bar) and low temperature (<4 °C) as exist in the oceans below upper slope depths. Their stability is also influenced by total salinity and presence of other gases in natural systems and by inhibitors and catalysts in technical systems. The top of the natural gas hydrate stability zone (GHSZ) along the global ocean margins is at water depths as shallow as 300 m in Arctic bottom waters and around 750 m in subtropical bottom waters. The base of the GHSZ varies with the water depth and the geothermal gradient and may range from 100s to 1,000s of meters below sea floor. In seep waters, high precision Cl-analyses, coupled with O- and D/H-isotopes of H_2O, may indicate the presence of gas hydrates in the subsurface that may drive seep flow (Matsumoto and Borowski 2000).

Biota and biomarkers

Function, structure and composition of seep biota and AOM-consortia in concert with biomarker are currently a major topic of seep research. The biomarkers are greatly depleted in ^{13}C relative to their carbon source and are linked to methanotrophic archaea (Elvert et al. 1999; Hinrichs et al. 1999; Rossel et al. 2008). This may result in isotopic compositions as low as −137 ‰ PDB (e.g., hydroxyarchaeol) depending whether biogenic or thermogenic methane is utilized. The nearly inexhaustible reservoir of methane carbon available to the consortia in seep environments maximizes the kinetic carbon isotope effect. Biomarkers from AOM-consortia are identified from sediments and authigenic carbonates of recent seep sites and increasingly from deposits of ancient seeps (Campbell et al. 2002; Nyman et al. 2010; Yang et al. 2011). So far, the oldest biomarker record was found in 300-million-year-old

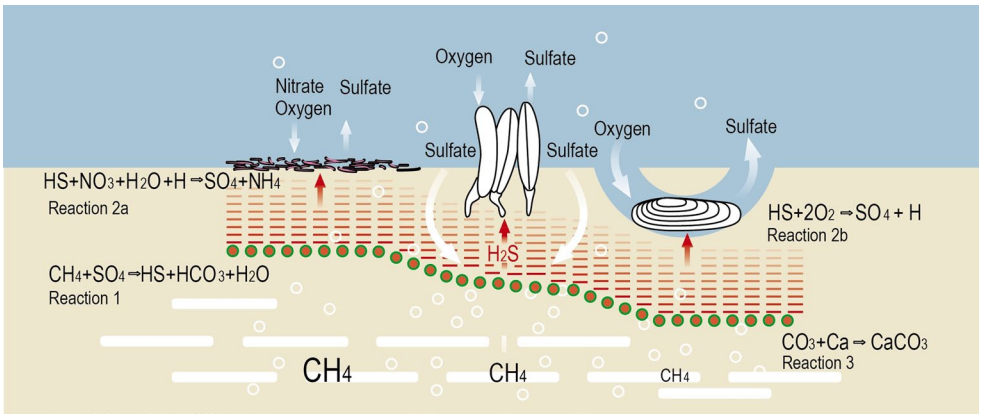

Fig. 7 Anaerobic oxidation of methane. Buried gas hydrates and free gas supply different rates of methane (*arrows*) to AOM-consortia (*red-green circles*) concentrated at distinct depths below seafloor. The consortia consume seawater sulfate in oxidizing methane (Reaction 1) producing hydrogen sulfide and bicarbonate; hydrogen sulfide rises to the sea floor and is oxidized in microbial mats (Reaction 2a) or by macrofauna symbionts (Reaction 2b) using oxygen or nitrate; in the process calcium carbonate precipitates (Reaction 3); from Suess and Linke (2006); see also Sahling et al. (2002) and Boetius and Wenzhöfer (2013)

limestone (Birgel et al. 2008). The library of biomarkers grows steadily (Rossel et al. 2008, 2011). Based on lipid analyses, three distinct AOM-consortia of ANaerobic MEthanotrophic (ANME-1, -2 and -3) archaea and their sulfate-reducing bacterial partners were tentatively identified as environmental indicators that respond to temperature, oxygen and sulfate availability (Rossel et al. 2011).

Benthic seep communities are highly visible, persistent and universal indicators for seep activity past and present. The dominant symbiotic taxa are tube worms, clams and mussels whereby different microbial consortia—mostly recognizable as brightly colored mats—provide carbon and energy via AOM. First publications of seep communities invariably noted the similarity of major taxa to those known from hydrothermal vents (Lonsdale 1979; Paull et al. 1984; Suess et al. 1985; Kennicutt et al. 1985). Numerous reviews and case studies since (Sibuet and Olu 1998; Sahling et al. 2002; Levin 2005; Olu-Le Roy et al. 2007; Kiel 2010) summarize vent taxa, document chemoautotrophy, follow energy and carbon flow, establish community structures, propose biogeographical provinces (Sahling et al. 2003; Baco et al. 2010; Zapata-Hernandez et al. 2013) and model interactions between seep fauna and for example microbial consortia (Cordes et al. 2007) or non-symbiotic mega-fauna (Niemann et al. 2013). Noteworthy, tube worms (pogonopherans), initially thought of as indicator organisms for abyssal environments (Ivanov 1963), remained unrecognized as members of the seep fauna until their distribution in deep-sea trenches could be related to convergent plate boundaries (Suess et al. 1985). New chemosynthetic species are continuously discovered at methane seep sites throughout the world (Hilario and Cunha 2008; Sellanes et al. 2008; Warén and Bouchet 2009; Sommer et al. 2009; Krylova and Sahling 2010; Pierre et al. 2014).

Typical members of seep biota from the Cost Rica and the Chile margin are also tubeworms (Fig. 8a, b), clams and mussels (Fig. 8e, f) and microbial mats (Fig. 8c, d). It is quite evident that the former is a sediment-starved environment, whereas the latter is heavily sedimented perhaps affecting the community structure. Zapata-Hernandez et al. (2013) suspect that the seep fauna off southern Chile constitutes a new biogeographical province as does Martin et al. (2010) for seep communities off New Zealand (Hikurangi subduction zone). Niemann et al. (2013) documented intake of AOM-derived food by non-symbiotic fauna (crabs) off Costa Rica based on ^{13}C-depleted fatty acids in stomach and muscle tissue that are identical to those of chemoautotrophic bacteria living there. On the other hand, it is doubtful that significantly ^{13}C-depleted foraminifera tests from seep sites at the Hikurangi margin and elsewhere result from chemoautothrophic intake of seep carbon by living forams. Rather they result from recrystallization of their tests in a ^{13}C-depleted environment (Martin et al. 2010; Torres et al. 2003). Equally, the colonization by cold water corals utilizing carbonate substrates at seep sites off New Zealand seems to be an accidental rather than a chemoautotrophic association (Jones et al. 2010; Liebetrau et al. 2010). A vast data collection with emphasis on chemoautotrophic biota was compiled in connection with the Census of Marine Life. The global effort of researchers from more than 80 nations engaged in a 10-year scientific initiative whereby mid-ocean ridges, hydrothermal vents and cold seeps are accorded special significance (Topics in Geobiology; Kiel 2010).

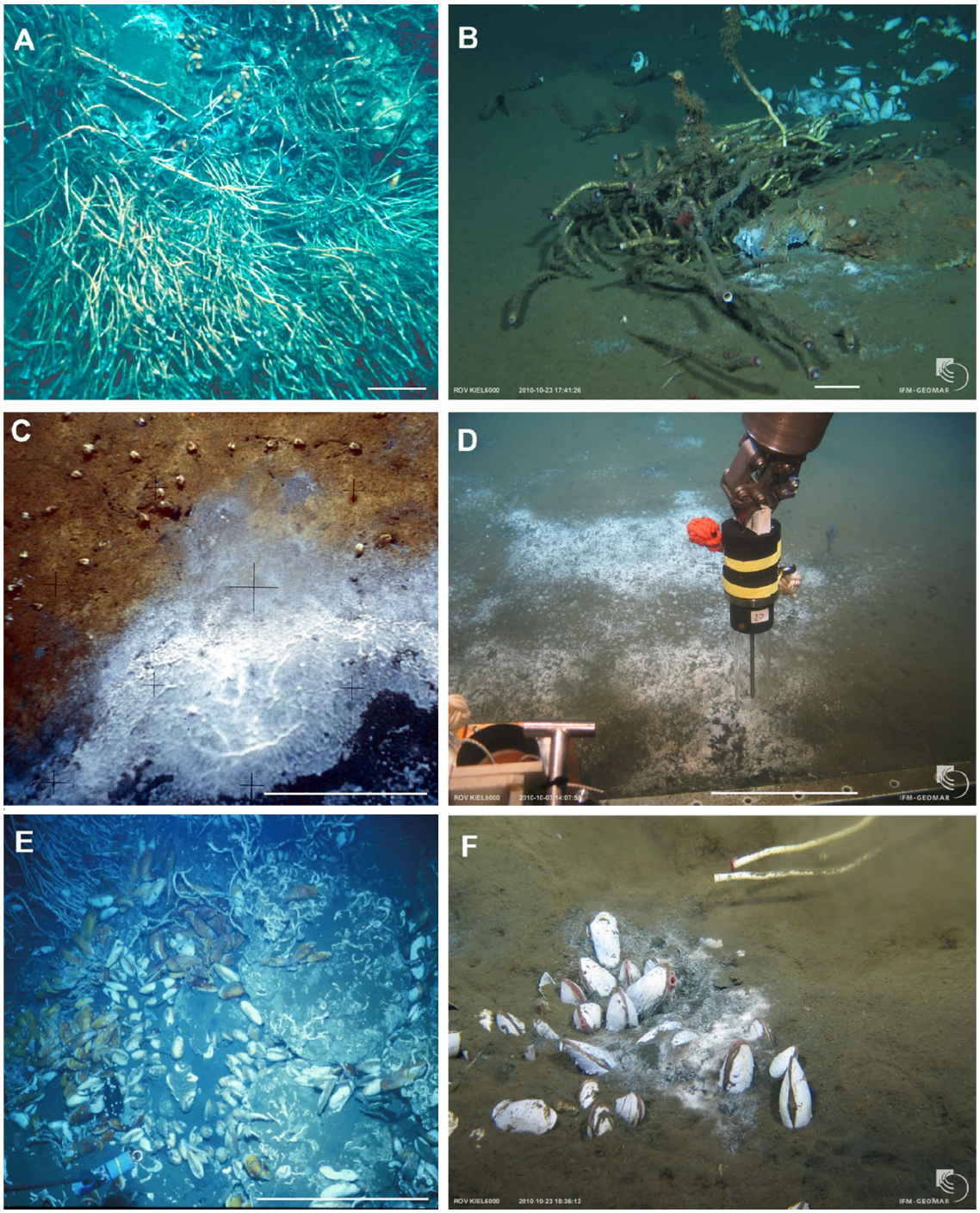

Fig. 8 Seep biota. Seafloor images of typical seep biota from the sedimented Chile accretionary margin (*right*) and the sediment-starved Costa Rica erosive margin (*left*). **a** Prolific Pogonophora colony from Jaco Scarp off Costa Rica; **b** pogonophora colony on seafloor off Conception, Chile; **c** varied microbial mats on seafloor of Quepos seep, Costa Rica; **d** microbial mat on smooth seafloor off Conception; **e** mytilid colonies on carbonates off Costa Rica; **f** vesicomyid colony on seafloor off Conception; photographs GEOMAR; Cruise Repts. SO163, Weinrebe and Flüh (2002); M54, Soeding et al. (2003); SO173, Flueh et al. (2004); SO210, Linke (2011)

Authigenic carbonates

A direct consequence of AOM is the precipitation of carbonate minerals. The association of carbonates with gas emissions, pockmarks and populations of chemosynthetic faunas is among the most widely used criteria to identify seeps. Carbonate buildups (chemoherms; Fig. 9a A, B) reaching several meters above the seafloor are believed to

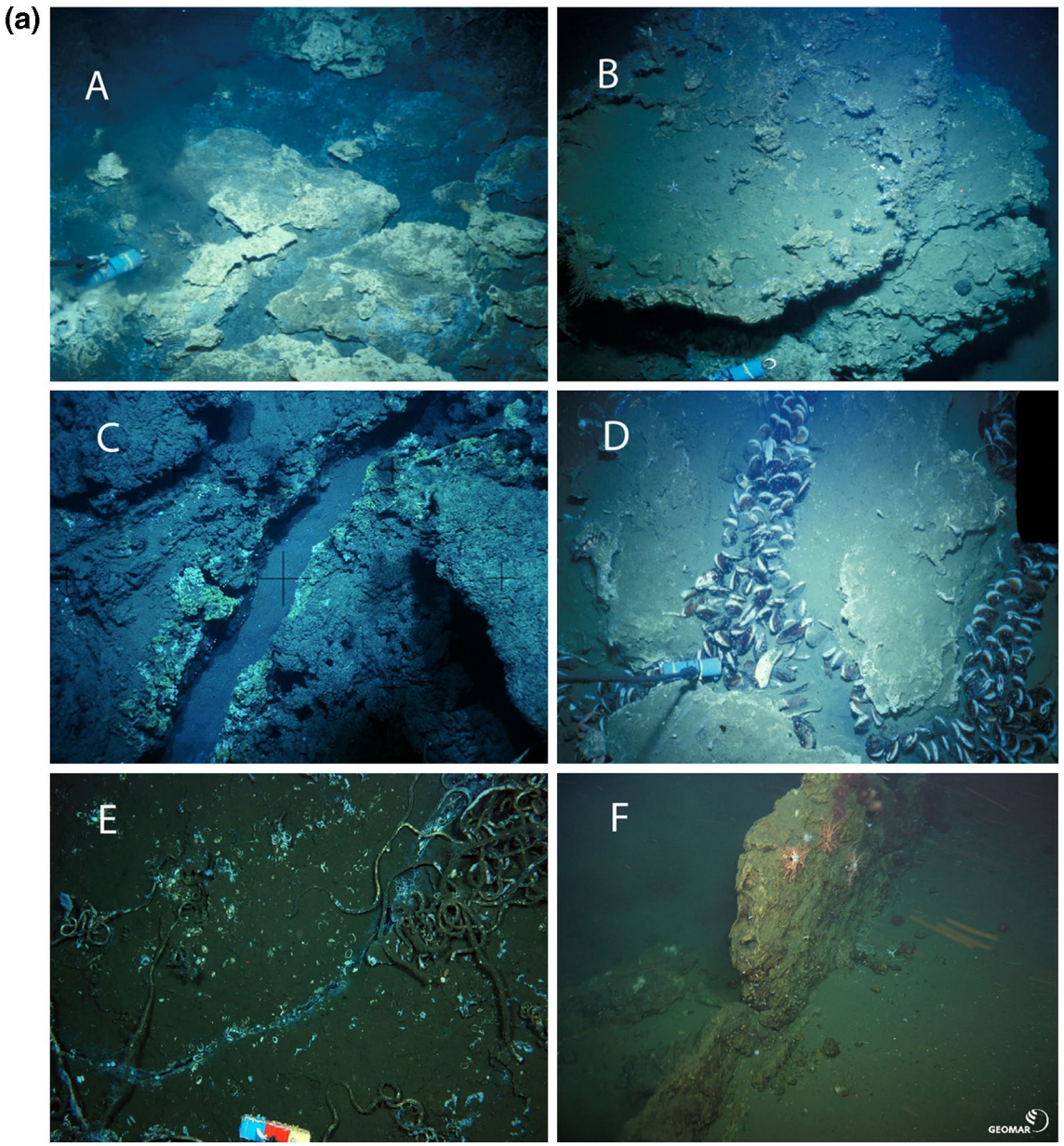

Fig. 9 **a** Seep carbonate structures. Seafloor images of typical seep carbonates. **A** Fractured block, Costa Rica margin; **B** chemoherm buildup populated by sessile organism, Costa Rica margin; **C** chemoherm buildup with micobial linings, South China Sea; **D** domed and fractured structure atop mud volcano with bivlaves, Costa Rica margin; **E** fractured pavement with tube worms and microbial linings, Chile margin; **F** uplifted and eroded block, Chile margin; photographs GEOMAR: Cruise Repts. M54, Soeding et al. (2003); SO173, Flueh et al. (2004); SO177, Suess (2005); SO210, Linke (2011). **b** Seep carbonate fabric. **A** Intergrowth of gas hydrate (*white*) and aragonite (*yellow*) in cemented mud matrix; Cascadia margin; **B** gas hydrate progressively disappears in minutes after recovery due to dissociation; **C** aragonite lining with imprinted gas hydrate fabric after complete dissociation; **D** chemoherm block with sessile organism and open fluid pathways, South China Sea; **E** aragonite linings of voids and open fluid channels; **F** network of open fluid channels in chempharm block; photographs GEOMAR: Cruise Repts. SO148, Bohrmann et al. (2000); SO177, Suess (2005)

form in contact with bottom water (Teichert et al. 2005; Han et al. 2004, 2008; Liebetrau et al. 2014). Other formations exist below the seafloor or are uplifted, exumed and eroded (Fig. 9a D). Typically, chemoherms incorporate shell fragments and have a network of open or cemented fluid channels that can be traced throughout the structure Fig. 9b D–F). Many other shapes and sizes of seep carbonates have been observed, too numerous to detail here. Recent publications note that (e.g., Han et al. 2008; Haas et al. 2010) the seafloor around seeps is often covered by blocky carbonates and fragments, irregular doughnut-shaped, tabular and tubular slabs and concretions with

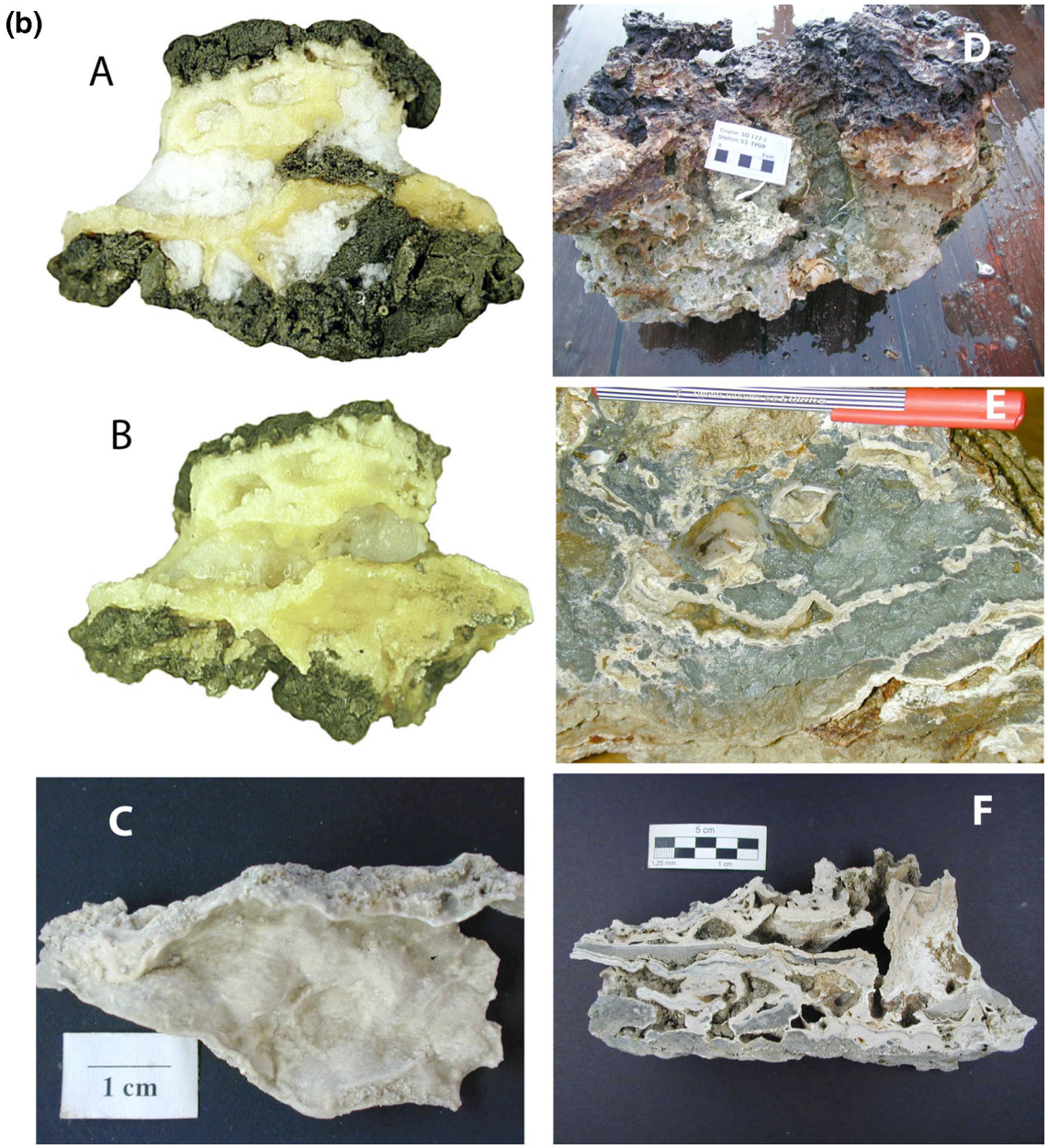

Fig. 9 continued

open or cemented central channels. Some appear to be molds of burrows or linings of fluid channels that formed in the sediment but resemble small chimneys after becoming exhumed by bottom currents. Pure carbonate (aragonite) layers are common that line voids or fill the conduits of near-surface concretions and chemohems (Fig. 9a E, F), whereas concretions deeper in the sediment that are fillings of burrows and molds most often consist of high-Mg-calcites (Han et al. 2008; Haas et al. 2010).

The dominant mineral phases are aragonite, Mg-calcite and (proto)-dolomite, but also Fe- and Mn-carbonates occur. Their $\delta^{13}C$ and $\delta^{18}O$ composition ranges from −60 to −30 ‰ PDB and +8 to +2 ‰ PDB, respectively, depending on the C- and O-source, the temperature and the specific mineral phases being formed (Bohrmann et al. 1998; Greinert et al. 2001; Teichert et al. 2005; Han et al. 2014; Mavromatis et al. 2012). Gas hydrate water, clay-dehydration water, glacial seawater and—in rare cases—meteoric water determine the O-isotope make-up, whereas biogenic, thermogenic and abiotic methane carbon, becoming strongly fractionated during AOM, determines the eventual C-isotope signal. The stable isotopes and the mineralogies are robust criteria, along with biomarkers for recognizing ancient seeps.

The characterization by stable C- and O-isotopes and mineralogies of seep carbonates now includes new geochemical, radiochemical and biochemical criteria to constrain absolute and relative ages, redox conditions of their environments of formation, trace elements to indicate sources and/or the types of fluid–sediment/rock interactions. These objectives may best be attained when pore or seep fluids are sampled at active seep sites along with the carbonate lithologies. This is not possible in all cases and—as it turns out—seep carbonates at active sites span a large time range that makes it difficult to assign any fluid or environmental signal to the solid product at any one time. Most promising advances come from lipid biomarker studies of AOM-consortia. Tentatively, the ANME-2/sulfate reducer cluster seems to favor both ambient bottom water temperature and oxygen conditions resulting in predominantly aragonitic phases in calcified mats, whereas the ANME-1 cluster favors elevated temperatures and diminished oxygen contents relative to ambient bottom water resulting in Mg-calcites (Haas et al. 2010; Rossel et al. 2011).

Seep footprint

Massive carbonate caps on mounds and pavements have been mapped as seep manifestations along continental margings. These are often fractured and heavily populated by seep biota attesting to ongoing seep activity (Fig. 9a C–E). Geo-acoustic tools (side-scan sonar, sub-bottom profiler) combined with high-resolution multibeam bathymetry not only serve to identify seep sites but are indispensable for quantification of seep fluxes. The acoustic seep signatures include smooth areas with slightly elevated backscatter intensity that result from high gas content or the presence of near-surface gas hydrates, to rough areas with widespread patches of carbonates at the seafloor thus providing a regional seep footprint as shown for the Costa Rica, Chile and Hikurangi margins (Sahling et al. 2008; Buerk et al. 2010; Klaucke et al. 2010, 2012). Ground-truthing by either video observations (Jones et al. 2010), flux measurements (Linke et al. 2005) and modeling of pore water profiles (Hensen et al. 2004; Karaca et al. 2012) provides the database from which to derive seep fluxes and reliably upscaling as shown in exemplary fashion for the Costa Rica margin (Freundt et al. 2014).

Nowhere does the need for accurate seep flux estimates become more evident than in the recent comparison between global seafloor oxygen consumption related to methane seepage (Boetius and Wenzhöfer 2013). The authors assuming "…a few tens of thousands of active cold seep systems on continental slopes worldwide…" find a significant mismatch between carbon lost from continental slopes globally and the maximum of methane that can be supplied via methanogenesis from within the topmost 1,000 m of Holocene sediments, primarily through seeps. This leads to the suggestion that "…a substantial fraction of the methane at seep systems is sourced from carbon buried kilometers under the seafloor." Admittedly, a more accurate estimate of global seep fluxes would not erase the mismatch, but the issue of a "deep carbon source" highlights the need for reliable seep flux estimates and up-scaling globally.

Age determination

Foremost among seep research is the age determination of authigenic carbonates. The first published U/Th-ages are from chemoherm samples of the Cascadia subduction zone (Teichert et al. 2003). The authors documented that methane-release events at seep sites largely occurred during low eustatic sea-level stands when lowered hydrostatic pressure falls below the sub-sea formation pressure. This initial interpretation is essentially confirmed as more age determinations become available. Among these are ages from seep carbonates of the Japan Sea going back 65 ky ago with all of six different ages coinciding with low sea levels (Watanabe et al. 2008). A compilation of 41 U/Th-ages (Feng et al. 2010) from the Gulf of Mexico, the Black Sea and the Congo fan shows seep carbonates forming from recent times through the last interglacial. Slightly, more dates fall around the Last Glacial Maximum, but the time span covered by these samples of the Congo fan appears too short for supporting the sea-level mechanism. At the Hikurangi margin, the youngest U/Th-ages measured so far are from several contemporary seeps around 2,100 ± 100 years ago (Liebetrau et al. 2010). Here, the geologic setting implies a margin-wide hydrological change controlling seepage.

From the passive margin seeps of the South China Sea, two sets of U/Th-ages have been published of which one (350 ky ago; Tong et al. 2013) coincides with high sea-level stand and another sample (11 ky ago; Han et al. 2014) coincides with rising sea level, whereas all others (16 samples) coincide with low sea-level stands. Other mechanisms have been discussed (Feng et al. 2010; Han et al. 2014) such as warming of bottom water that destabilizes methane hydrate, increase in the sediment loading, salt diapirism or erosion of the seafloor or tectonism at active margins; all of which could force methane from the sediment.

Periods of low sea-level stands do not exclusively favor methane-release events as there is currently—at high sea level—vigorous seepage at large carbonate structures that have had a long history. Recently, Crutchley et al. (2013) have shown by numerical fluid simulations an increase in water–gas fluid accumulation below the base of the gas hydrate stability that underlies a long-lived vigorously seeping carbonate structure, the Pinnacle. This is a >50 m high chemoherm at the Cascadia subduction zone. The site

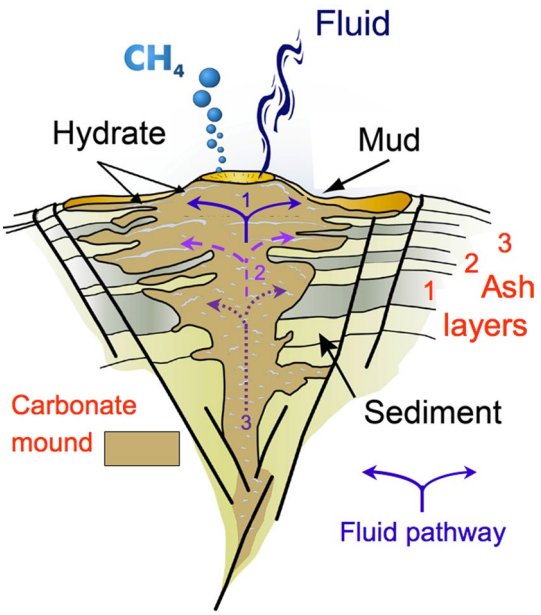

Fig. 10 Generic mud volcano with core of carbonate mound. Mud, methane and fluids are emitting while carbonates and interlayered hydrate form, whereas sediment and ash layers alternate along flanks. A normal sequence of ash layers (1–3) records lifetime and cyclicity of venting. The sequence of carbonate ages (1–3) if reversed (top = older than bottom) results from plugging of fluid pathways; based on Kutterolf et al. (2008) and Liebetrau et al. (2014)

of water–gas fluid accumulation at depth is a distinct lithologic boundary that constricts flow. The resulting overpressure forces methane continuously through a well-defined network of faults to the Pinnacle site regardless of sealevel.

First-of-its-kind investigations of intercalated carbonate and host sediment on flanks of seep structures and of drill cores taken in the centers of mud volcanoes on the Costa Rica margin (Kutterolf et al. 2008; Liebetrau et al. 2014) revealed at first sight unconventional results. The mud volcanoes grew through several active phases with ash layers providing time markers (6, 17, 24.5, 69, 84 ky ago) and carbonates the U/Th-ages (ranging from 5 to 65 ky ago). Ages of the drill core samples through the carbonate cores of the structures showed downward progression of growth instead of upward as the ages of the mounds do with inward growth instead of outward (Liebetrau et al. 2014). Both trends are readily explained by plugging of the fluid pathway with time by authigenic carbonate precipitation. The internal structure of a generic mud volcano with an authigenic carbonate core (Fig. 10) shows intercalated muds and volcanic ash layers that were dated to provide the lifetime and cyclicity of seep activity. The apparently reverse U-/Th-ages result from sequential plugging of older fluid pathways by carbonate precipitation on top of the structure and the younger carbonates forming near the bottom as illustrated in Fig. 10. Though, globally and over Quaternary times, eustatic sea-level fluctuations are currently favored to control the activity of the numerous less vigorous seeps.

Fluid–sediment interaction

There has been a long-standing and religiously performed analytical procedure on pore water chloride contents with little disagreement about the accuracy by the Deep Sea Drilling Project and its successors. Many 1,000s of interstitial Cl-profiles in drill cores have been established documenting endless deviations—enrichment as well as depletion—relative to seawater chloride. All of these are expressions of fluid–sediment interaction, mostly 100s of meters below the sea floor. In seep settings, these familiar Cl-anomalies along with those of trace constituents are compressed in concentration-depth profiles toward the sediment–water interface by upward fluid flow. Sometimes the anomalous fluids are emitted to the free bottom water where they may or may not be recorded by the hydrocarbon–microbes–metazoan–carbonate association.

Gas hydrate water Much attention has been focused on Cl-anomalies from the release of methane hydrate water. This anomaly is an artifact of sampling as removal of drill cores from in situ temperature and pressures destabilizes gas hydrate phases in the sediment. Coupled with O- and D/H-isotopes of H_2O, the resulting anomalies may be linked to gas hydrates and indeed are widely used to estimate the hydrate saturation of deposits (Matsumoto and Borowski 2000; Haeckel et al. 2004; and many others). Release of hydrate water is restricted to layers at and above the bottom simulating reflector (BSR) diluting the Cl-concentration and increasing the $\delta^{18}O_{H_2O}$ of pore fluids (Fig. 11).

Seep carbonates being precipitated during AOM are another sink of $\delta^{18}O_{H_2O}$ from hydrate water. This was first shown in an aragonite–Mg–calcite intergrowth retrieved form seeps at the Cascadia convergent margin (Bohrmann et al. 1998). The C-isotope ratio ($\delta^{13}C = -40$ to -54 ‰ PDB) of this intergrowth (Fig. 9b A, B) identifies both mineral phases as being derived from biogenic methane. As the aragonite—the younger phase—was shown to have formed in equilibrium with ambient bottom water temperature, the Mg-calcite—the older phase—was enriched in $\delta^{18}O$ by about +1 ‰ PDB. This is attributed to gas hydrate water in the precipitating fluid. Hydrate water may be enriched in ^{18}O of up to 3.5 ‰ PDB (Maekawa 2004). The lining of the carbonates in contact with the hydrate images the hydrate morphology (Fig. 9b C) and further supports the transfer of "heavy" ^{18}O from hydrate waters to carbonates. The term "clathrite" was proposed for this type of rock, invoking "clathrate" the family of water-caged gases. The name did not stick but what stuck is the interpretation

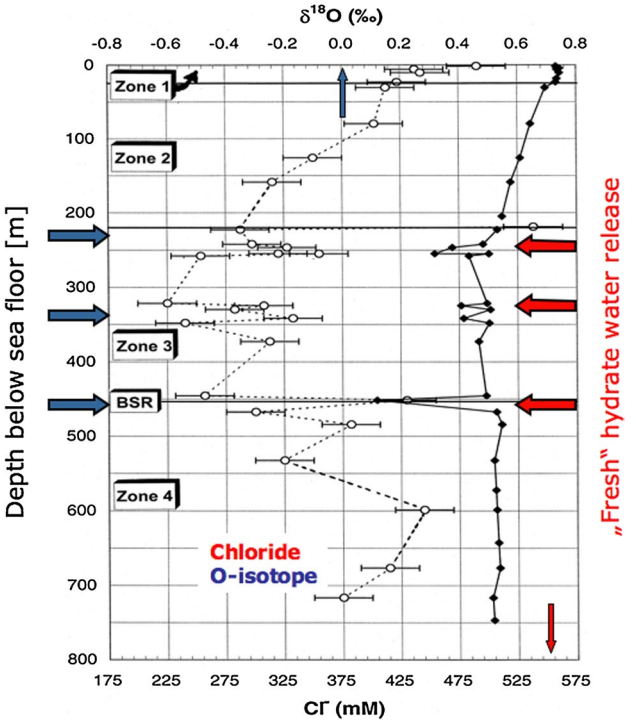

Fig. 11 Hydrate water in pore fluids. Well-known artifact of dissociating gas hydrates in drill cores by warming after retrieval; release of hydrate water dilutes Cl-concentration and increases $\delta^{18}O_{H_2O}$ of pore fluids; from Matsumoto and Borowski (2000)

of "heavy" δ^{18}O-values of seep carbonates as sourced by methane hydrate. Currently, many reports of "heavy" δ^{18}O-values of seep carbonates are linked to methane hydrates in the subsurface (Tong et al. 2013; Lu et al. 2005; Han et al. 2004; Matsumoto 1989) although there are other sources of "heavy" water being emitted at seeps (Dählmann and de Lange 2003; Hensen et al. 2004).

Clay dehydration Trioctahedral clays (smectite group) lose interlayer water in three steps to form illite responding to temperatures and pressures that prevail at the plate interface in subduction zones (80–120 °C). This was experimentally shown by Colten-Bradley (1987) and since by many others. Depending on the percentage of smectites, dehydration generates considerable amounts of fresh water, affecting interstitial chloride contents (Saffer and McKiernan 2009). Incomplete dehydration changes 18 Å- to 15 Å-smectite by releasing water without forming illite. The expression of clay-dehydration either at complete or incomplete conversion to illite is evident on a large scale in Cl-dilution of pore fluids of accretionary margins. For example, data from ten drill sites across the Cascadia subduction zone (Torres et al. 2004) show progressive freshening attributable to increased compaction and smectite–illite transformation (Fig. 12). Sites at the accretionary prism (Stations 1245–1247) show Cl-dilution at 150 m below seafloor and above the BSR depth from dissociation of gas hydrate.

The δD (−32 ‰ SMOW) and δ^{18}O (+10 ‰ SMOW) of interlayer water differ significantly from those of seawater as determined for deeply buried strata of mud volcanoes (Dählmann and de Lange 2003). These isotope characteristics affect the pore water δD and δ^{18}O upon dehydration. In addition, trace elements sorbed in the interlayer space or external clay surfaces are also affected by clay dehydration as for example with boron and lithium.

Significant boron enrichment with diluted Cl-contents in pore fluids from seep sites (mud volcanoes) off Costa Rica and the δD and δ^{18}O isotope ratios of seep water is attributed to clay dehydration (Fig. 13; Hensen et al. 2004). The desorption of boron from smectites is temperature dependent (complete at 100 °C), and thus, for the first time, it was established that fluids originate 1,000s of meters below the seafloor—preserving a signal of sediment–fluid interaction—and transport it through the backstop rocks of the overriding plate (Ranero et al. 2008). The transport is facilitated and in concert with lithic material that constitutes the mud volcanoes but is rarely examined in detail.

Lithium, a widely used tracer of water–sediment interactions, has been investigated experimentally for temperatures between 70 and 150 °C. This range prevails at the plate interface of subducting margins (Decarreau et al. 2012). In smectites, magnesium is replaced by lithium in the octahedral layer (hectorite, swinfordite). This reaction is favored by increased Li-content of the fluid and increased temperature. Hence, authigenic smectites may be efficient Li-sinks, and equally, dehydration of Li-smectites is expected to be a source of lithium. Scholz et al. (2009, 2010) established a widely applicable relationship between Li-content and δ^7Li for fluid–sediment interaction (Fig. 14). This relationship is based on a large dataset of pore fluids from different diagenetic regimes involving different host sediments. Basically, it characterizes the following regimes: (1) low- and (2) high-temperature diagenesis and (3) ridge-crest and (4) sediment-hosted hydrothermal systems. Significantly, seep fluids associated with mud volcanoes of the Mediterranean Ridge and the Golf of Cadiz show characteristics of the high-temperature regime, those of the Golf of Cadiz even of fluid–sediment interaction at hydrothermal regimes (>200 °C; Scholz et al. 2009). This attests to the fluid signal acquired 1,000s of meters below the seafloor; e.g., release of Li at high temperatures and uptake during illitization of smectite. Seep fluids from mud extrusions of the Nile delta and the Central American subduction zone exhibit characteristics related to provenance; in the one case, weathered low Li-sediments are delivered and in the other high-Li-volcano clastics.

Strontium and its ^{87}Sr/^{86}Sr isotope ratio provide another set of signals related to fluid–sediment and rock interaction.

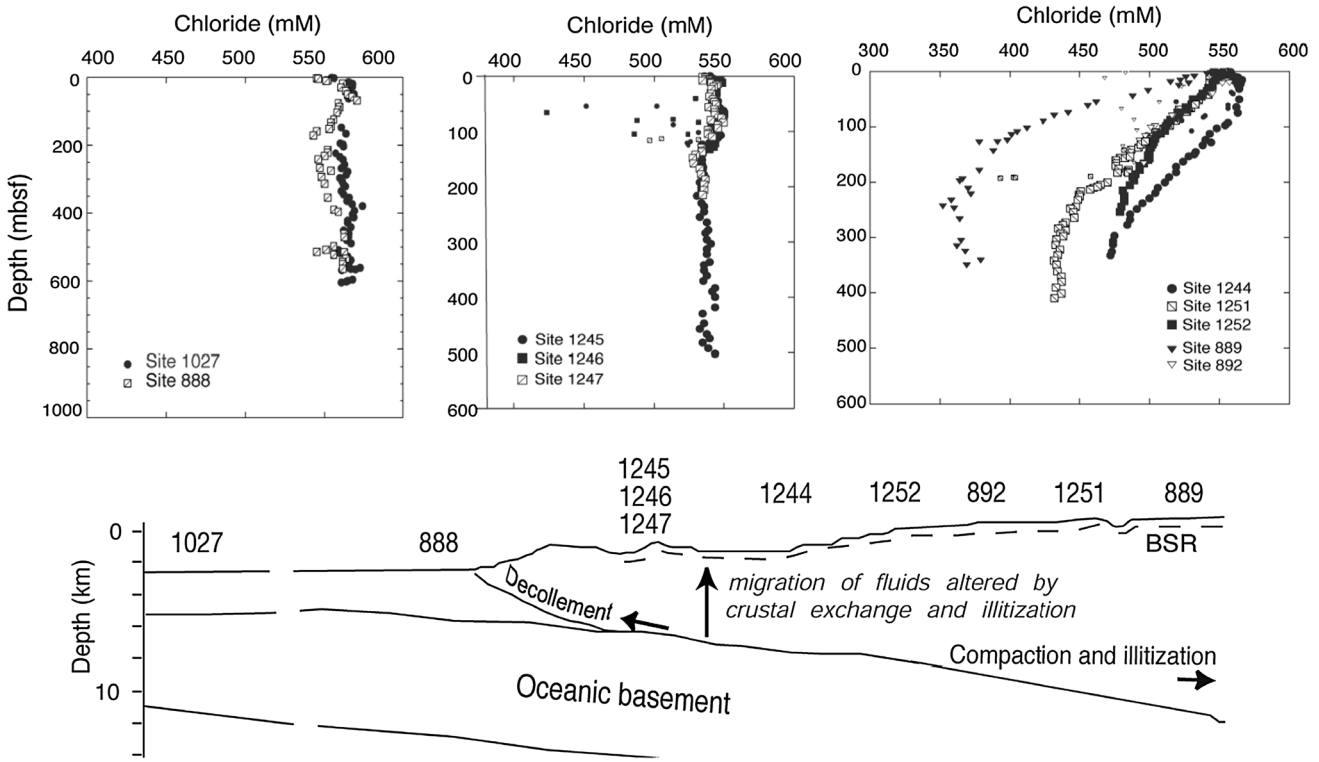

Fig. 12 Clay dehydration. Chloride dilution in pore fluids of accretionary margins from deformation front toward continental framework rock is observed worldwide in ODP-drill sites. Data from ten sites across the Cascadia margin show progressive freshening attributed to increased compaction and smectite–illite transformation. Sites at the accretionary prism (Stations 1245–1247) show Cl-dilution <150 m below seafloor and >BSR depth from dissociation of gas hydrate; modified from Torres et al. (2004)

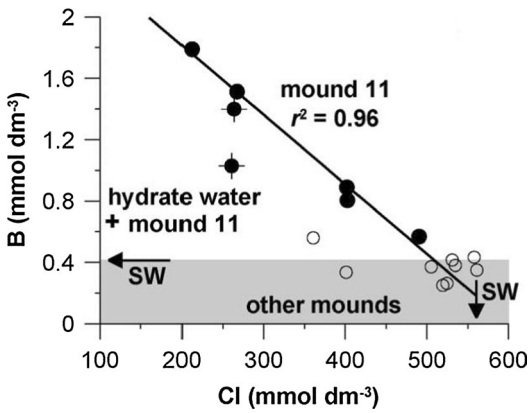

Fig. 13 Boron as tracer for clay-dehydration water. Seeping of clay-dehydration water from active mud volcanoes off Costa Rica with B-enrichment and strong Cl-dilution; release of hydrate water as cause for Cl-dilution is excluded and temperature of dehydration (~85 °C) derived from $\delta^{18}O_{H_2O}$ and δD_{H_2O} (not shown here). SW = concentration in seawater; modified from Hensen et al. (2004)

Release of radiogenic strontium (high $^{87}Sr/^{86}Sr$ ~ 0.7149) from terrigenous sediment to pore and seep fluids represent one end-member component and low radiogenic strontium (low $^{87}Sr/^{86}Sr$ ~ 0.7029) from the oceanic crust and basalt the other. Both end-members are affected –through time- by changing seawater strontium (Quaternary [high] $^{87}Sr/^{86}Sr$ = 0.7091; Cretaceous/Jurrasic [low] = 0.7068 (Burke et al. 1982). As boron and lithium provide better temperature records of interaction, authigenesis and dehydration, strontium seems better suited as source indicator. This is true for seep fluids from the oceanic basement and volcanic clastics. Continental volcanics contain a small proportion of radiogenic strontium ($^{87}Sr/^{86}Sr$ from 0.7072 to 0.7082).

Seep and pore fluids from mud volcanoes across the Golf of Cadiz (Scholz et al. 2009) record the evolution from high radiogenic strontium leached from terrigenous clays of the accretionary prism located close to land (eastern Golf of Cadiz) to basement-derived fluids farther away at the margin of the prism (western Golf of Cadiz; Fig. 15). Remarkably, one set of mud volcanoes is located along the northern branch of a transform fault system that crosses the accretionary prism from E–W and the other set located along a southern branch. Both sets show coincident progressive change from continental runoff (sediments of the accretionary prism) toward hydrothermal exchange (underlying oceanic crust) with distance. By extension, outside the accretionary prism, largely basement-derived

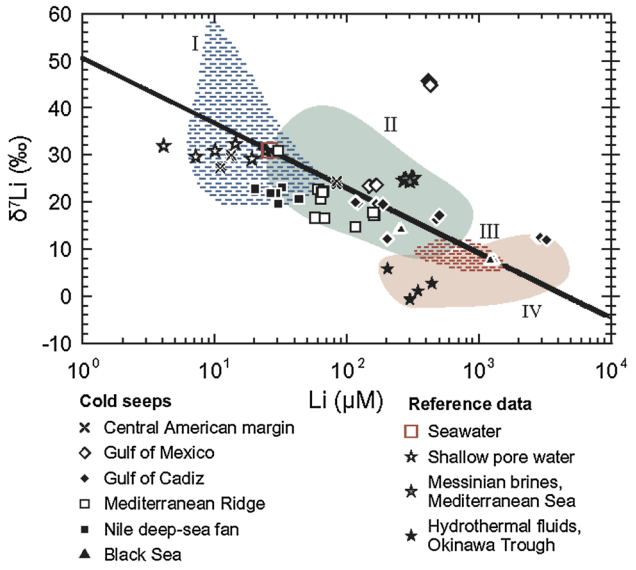

Fig. 14 Lithium tracer for fluid–sediment reactions. Based on reference data of Li and δ^7Li relationships (partially listed in the legend), several domains of fluid–sediment interaction are evident: (*I*) low-temperature diagenesis, (*II*) high-temperature diagenesis, (*III*) ridge-crest hydrothermal systems and (*IV*) sediment-hosted hydrothermal systems. Superimposed seep fluids from convergent, transform and passive margins show such source signals or differing signals depending on host sediments; modified from Scholz et al. (2010)

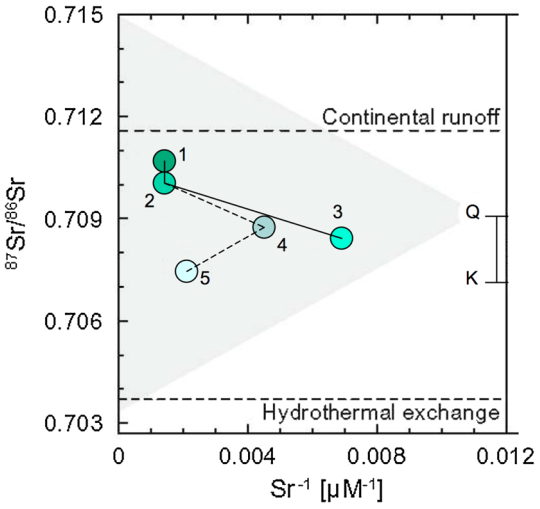

Fig. 15 Strontium tracer for deep fluids. Sr and $^{87}Sr/^{86}Sr$ relationship in seep and pore fluids from mud volcanoes in the Golf of Cadiz. Mud volcanoes #1–3 are located along a northern transform fault that crosses the accretionary prism from E–W and mud volcanoes #1, 4–5 are located along a southern transform fault. Both show progressive change from continental runoff (sediments of the accretionary prism) toward hydrothermal exchange (underlying oceanic crust) with distance. Such signals in seep fluids may be regarded as criteria for transform fault systems. Sr-isotopic characteristics for current (Q = Quaternary) and past (K = Cretaceous) seawater; modified from Scholz et al. (2009)

fluids are to be expected. The injection of basement fluid is likely driven by strike-slip motion and simultaneous thrusting along deep-rooted faults of the African–Eurasian plate boundary (Gutscher et al. 2012).

Submarine silicate weathering Reactions of poorly weathered sediments with pore fluids in continental margin sediments has been recognized as impacting pore water compositions (Aloisi et al. 2004a; Wallmann et al. 2008; Scholz et al. 2013). Hereby, submarine silicate weathering continues to form smectitic phases from cations, alkalinity and silica. In the process, water is taken up and increases the chloride content of the pore fluids. Although no such Cl-enriched fluids have been observed seeping from the seafloor above the accretionary prism off central Chile or other margins, the authors (Scholz et al. 2013) argue that water uptake by smectite formation and water release by smectite–illite transformation might compensate each other to a degree that makes documentation difficult. At this point, it should be recognized that continued submarine silicate weathering is an important post-depositional process that is probably more prevalent in buried continental margin pore fluids as it is in seep fluids emitted at the seafloor along margins.

Redox conditions The few datasets of REE pattern and trace metals (V, U, Mo) available from seep carbonates might be used as redox indicators (Ge et al. 2010; Himmler et al. 2010; Rongemaille et al. 2011; Bayon et al. 2011). The basis for interpreting trace metal and REE patterns is that these elements have multiple oxidation states and that a transition may be accompanied by a change in solubility in seawater, hence fixation of insoluble species during seep carbonate precipitation; e.g., for Ce as CeO_2. Samples from passive margin settings exhibit a range in Ce-anomaly pattern [=log (Ce/Ce*) between 1.19 (oxic environment] and <1 (anoxic environment) tentatively assigning redox conditions during seep carbonate formation. In some cases, the V, Mo and U concentrations (e.g., U = highly insoluble under anoxic conditions) vary in accordance with the Ce-anomalies. Overall though, the redox characterization at present seems weak or inconclusive as several authors point to the need for improved extraction procedures to reduce contamination, better knowledge about REE-partitioning among the carbonate phases, and advantage of micro-scale determination [laser ablation-inductively coupled plasma-mass spectrometry (LA-ICP-MS)] to detect changes in formation fluid from which the carbonates precipitated (Rongemaille et al. 2011; Himmler et al. 2010). Though some promising criteria have emerged in that aragonite more faithfully preserves fluid REE pattern at bottom water conditions and that strong enrichment of the MREE pattern (normalized to Post-Archaean Australian Shale) indicates a deep-sourced signal,

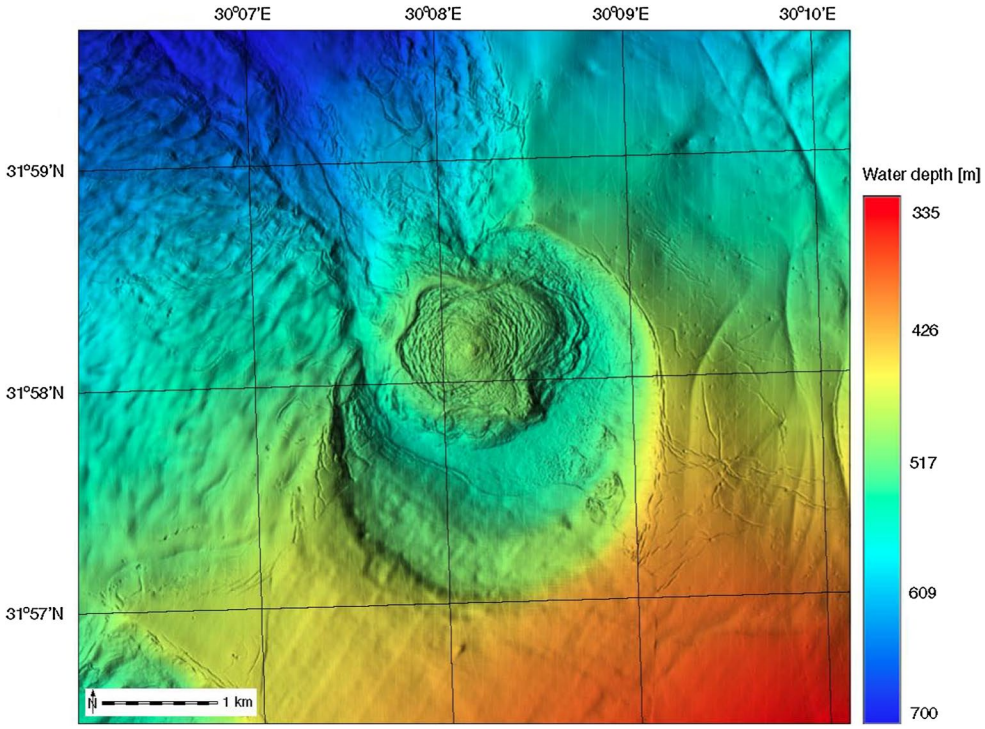

Fig. 16 Nile deep-sea fan. *Shaded* bathymetric map of the North Alex Mud Volcano with mud ponding, breached crater rim and outflow structures; modified from Feseker et al. (2010); map DTM courtesy BP Ltd)

whereas Bayon et al. (2011) emphasize that REEs emitted by seep fluids are scavenged by Fe–Mn-oxyhydroxides and that authigenic precipitates do not record any REE-signal other than that of seawater based on εNd values. In contrast, a significant step in understanding REE pattern comes from pore waters of cold seep sediments from Hydrate Ridge (Himmler et al. 2013). High total dissolved REEs seem to become mobilized from remineralization of organic matter in the active AOM-depth interval. Here, formation of carbonates consumes calcium and REEs, which highlights the great potential to constrain environmental conditions from REEs in seep carbonates.

Unique seep settings

Among the geologic settings that generate seeps are those that accumulate organic-rich sediments in basins, in deltas, and those that are underlain by evaporites and hydrocarbon reservoirs. They provide unique characteristics expressed in mud volcanoes, pockmarks, brine lakes and—as with all seep settings—in authigenic carbonates. The Gulf of Mexico, the eastern Mediterranean Sea including the Nile deep-sea fan, the Black Sea, the South China Sea and the deltas of the rivers Congo, Niger and Mississippi all have been extensively investigated. Focus of the most recent investigation is the Atlantic coast off North America.

Seeps associated with evaporites are generated from underlying salt strata where loading by sediments causes salt to flow forming salt domes and salt ridges. Hereby, low-density and low-viscosity salts escape the pressure of overburden by flowing upward. Salt domes push through the overlying strata, dragging them upward thereby developing faults along their flanks. This facilitates migration of fluids and in most cases liquid hydrocarbons. The tops of salt domes, near the seafloor, often dissolve away by circulating seawater and collapse. The result is large pockmarks, resembling the circumference of the underlying salt dome. Some contain brine pools and significant amounts of non-methane hydrocarbons including asphalt (MacDonald et al. 2004). The shelves and slopes surrounding the Gulf of Mexico contain such seeps and pockmarks related to salt tectonics as does the seafloor of the slope off Yucatan and have been the sites of extensive investigation (Roberts and Boland 2010). These are important provinces of oil and gas exploration and of classical hydrocarbon seep studies (MacDonald et al. 1990; Sassen et al. 2004).

The Messinian salt underlying the Mediterranean Sea affects fluid movement in the Nile deep-sea fan (Loncke et al. 2006). Seeps, mud volcanoes, methane plumes, carbonates and microbes have been reported there (Dupré et al. 2007; Gontharet et al. 2007; Feseker et al. 2010). Two prominent mud volcanoes (>50 km in diameter) with high temperatures (≫50° a few meters below seafloor) extrude muds and fluid, strongly depleted interstitial chloride and contain thermogenic gases (Figs. 16, 17). The mud surface appears wrinkled with ponding and outflow structures where the rim is breached. Currently they appear to be moderately to highly active (Feseker et al. 2010).

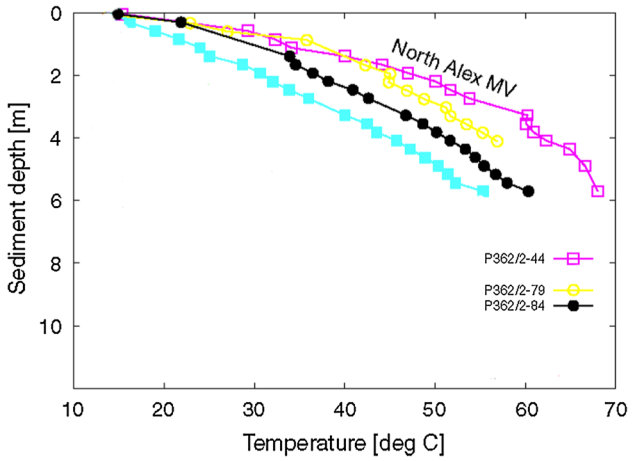

Fig. 17 Mud volcano near-surface temperature. In situ sediment temperature profiles from the center of North Alex Mud Volcano; strong increase to >60 °C attests to strong activity and mud extrusion from depth; modified from Feseker et al. (2010)

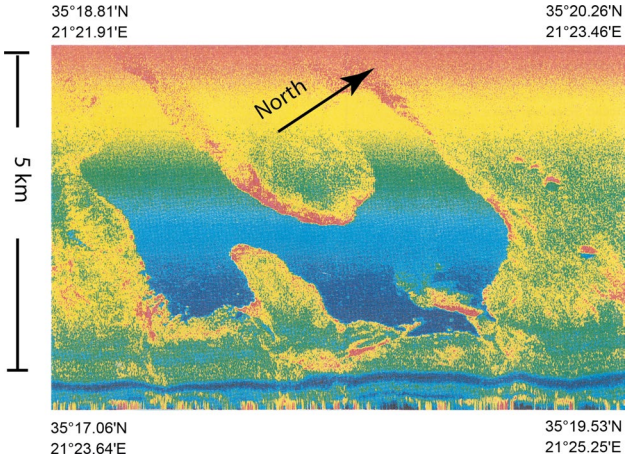

Fig. 18 L'Atalante brine lake. False-color side-scan sonar image shows horse shoe-shaped brine lake on the Mediterranean Ridge; modified from Suess and Linke (2006) based on Westbrook and MEDRIFF Consortium (1995)

Quite similar features have been recorded for the Håkon Mosby mud volcano on the slope of the Barents Sea with a >300 ky history of extrusion (Perez-Garcia et al. 2009). Ongoing activity has produced flow structures inside the crater evident in subtle morphological changes recorded by high-resolution seabed mapping over a 3-year period (Foucher et al. 2010). Even though large amounts of hydrocarbon gasses are emitted, the elevated mud temperature of currently active mounds prevent gas hydrates from forming entirely—as with those on the Nile deep sea—or only around the margins where temperatures are low as with Håkon Mosby mud volcano (Feseker et al. 2008).

This is different along the subduction zone of the eastern Mediterranean Sea—the Mediterranean Ridge. Here at the intersection of the Hellenic and Cyprus arcs lies the Anaximander Mountain region, the Olimpi area of mud volcanoes (Limonov et al. 1996; Aloisi et al. 2000; Pape et al. 2010) with extensive gas hydrate and brine lakes (Westbrook and Reston 2002). The driving mechanism for seepage and mud extrusion is the convergence of the African and Eurasian plates whereby the Messinian evaporites impart their composition on the hydrocarbon–metazoan–microbe–carbonate association (Olu-Le Roy et al. 2004; Pancost et al. 2000). Most noteworthy are brine pools at the seafloor (2,000–3,000 m) at the western part of the accretionary wedge where the morphology is controlled by convergent tectonic (Camerlenghi et al. 1995). The brines are at or close to saturation with respect to chlorides of sodium, magnesium and potassium (Fig. 18). The composition varies significantly between adjacent pools and depends on the depths within the salt sequence from which the fluid is generated (Westbrook and MEDRIFF Consortium 1995).

In the Golf of Cadiz, an accretionary wedge partially underlain by evaporites and cut by a transform fault system combine to generate complex expressions of seepage and mud extrusion (Gutscher et al. 2012; León et al. 2012). Few of the mounds are currently active, harbor seep biota (Sommer et al. 2009) and are thought to experience thermal pulses and injection of brine (Haffert et al. 2013). The composition and source of fluids and muds are controlled by terrigenous continental characteristics in the landward part of the complex changing to oceanic crustal characteristics seaward (Hensen et al. 2007). Fluid–sediment and rock interactions convincingly document this trend (Scholz et al. 2009).

The Black Sea has been accorded special effort in ongoing seep studies for its anoxic, methane-rich water column below about 100 m and its thick, up to 16 km, organic-rich sediments (Bohrmann et al. 2003; Mazzini et al. 2008). Over 2000 seeps were mapped off Romania and the Ukraine (Naudts et al. 2006). The sites are concentrated at the shelf-slope break extending to about 725 m water depth. In the sub-seafloor below that water depth, the stability limit of methane hydrates has been projected from the bottom water temperature and the geothermal gradient implying that above 725 m gaseous methane escapes into the bottom water and below, methane is retained as hydrate. The seep province continues off the Crimean Peninsula where in the eastern basin, gas hydrates, methane plumes in the water column and mud volcanoes at 1,000–2,300 m depth were discovered (Greinert et al. 2006). Still farther east at the margin off Georgia, extensive methane seepage is found in the Batumi area where state-of-the-art pressure coring technology was used to quantify methane emissions and subsurface gas hydrate (Pape et al. 2011; Heeschen

et al. 2011). Throughout the Black Sea authigenic carbonates of many morphologies and compositions are associated with the seep provinces although seep macrofauna appears to be absent. Instead, microbial communities, mats and microbial reefs abound (Peckmann et al. 2001; Treude et al. 2007). Several new discoveries of seeps and ongoing research from other known sites on passive margins are likely to expand the criteria for characterizing the hydrocarbon–metazoan–microbe–carbonate association.

In the South China Sea, basin-wide seep activity is concentrated in active and passive margin settings. Along the accretionary prism that results from plate subduction at the Manila Trench off Taiwan Island, methane seeps are common (Huang et al. 2006; Lin et al. 2008; Schnürle et al. 2011). The westward transition toward a fully passive margin setting reveals equally active seeps (Suess 2005). Their manifestations are largely authigenic carbonates with biomarkers, REEs, U/Th-ages and carbonate mineralogies having all been investigated in detail (Chen et al. 2005; Lu et al. 2005; Han et al. 2008). The timing of methane-release events primarily during low sealevel stands (Feng et al. 2010; Tong et al. 2013; Han et al. 2014) and the possibile recording of oxic or anoxic conditions during carbonate precipitation are currently under discussion (Ge et al. 2010). Other finds are reported from the Congo deep-sea fan (Kasten et al. 2012) with research on authigenic carbonates and associated biota in progress (Pierre et al. 2014).

A most recent survey of the water column and the seafloor along the Atlantic margin off North America with an advanced multibeam sonar system aboard the NOAA ship Okeanos Explorer showed methane plumes in 40 locations (NOAA ref. 2013). The subsequent Deepwater Canyons 2013 Expedition (NOAA-OER/BOEM/USGS) documented all manifestations of cold seepage of which the images of "creepy crawlies" attracted the most media attention so far.

Seep characteristics from erosive and transform margins

No previous attempts are known for characterizing the seep fluids emitted at erosive and transform margins in their own right, although some specific properties stand out. As higher temperatures and pressures and portions of the down-going plate are involved, mineral-bound water from opal or clays, and elements susceptible to mobilization under these conditions are added to the upward flow. Mineral-bound water dilutes the salinity of the seep fluid. It is characteristically ^{18}O-enriched and contains mobilized elements as boron and lithium (Chan and Kastner 2000; Dählmann and de Lange 2003; Hensen et al. 2004; Scholz et al. 2010).

At still higher pressures and temperatures, serpentinization sets in. During these reactions, methane is formed from reduction of oceanic carbon dioxide by hydrogen which in turn is released from common olivine reacting with seawater. Basically, the dissolution of mixed Mg-, Ca-silicates containing Fe (fosterite, enstatite, fayalite) initially results in high-pH waters forming cations and aqueous silica. These in turn react to form suites of serpentinite minerals (chrysotile, serpentine), hematite and molecular hydrogen. Further reactions, e.g., of hydrogen with dissolved carbonate ions of seawater form abiotic hydrocarbons largely methane and of high-pH waters with seawater form authigenic carbonates. Free hydrogen that is not consumed by CO_2 reduction is abundant at serpentinization-driven seeps as are archaea thriving at pH values of >12 (Mottl et al. 2003).

Mud volcanoes are seafloor manifestations of deep-sourced seeps on erosive margins. At the Mariana Fore-Arc and the Costa Rica margin, they are aligned above sub-seafloor isotherms (Mottl et al. 2004; Ranero and von Huene 2000; Ranero et al. 2008). Hence, their geochemical and isotope characteristics provide good evidence for depths and temperature of fluid generation. Not just fluids are expelled at mud volcanoes but also solids from the conduit walls. Unfortunately, studying these lithic products is not fully taken advantage of. Besides establishing the stratigraphy and composition through which fluids pass, the material may also transport microbial life from the deep biosphere to the seafloor.

Fluids from transform margins are derived from great depth because steeply dipping and deep-reaching fault planes are common for transform fault systems. As with seep fluids, however, and with mud volcanoes in any tectonic setting the nature and provenance of the sediment sequence through which the fluids ascend will impart their characteristics to the fluids and thus mask any deep-source signal. The pore and seep fluids from the North Anatolian Transform in the Marmara Sea have a brackish water source among others and have experienced a diversity of reactions (Zitter et al. 2008; Tryon et al. 2010) with no clear transform fault indicator. Fluids from the Gulf of Cadiz that ascend through evaporites are clearly characterized by their halite, gypsum and late-stage evaporite salt contributions (Hensen et al. 2007; Haffert et al. 2013). Barium in fluids and barites from the Derugin Basin (Sakhalin Transform system; Greinert et al. 2002) the San Clemente Fault (San Andrea Transform system; Torres et al. 2002; McQuay et al. 2008) as well as among the precipitates from the North Aantolian fault system (Crémiere et al. 2012), initially thought to be unique to transform settings (Suess 2010), are now thought to originate from non-detrital biogenic barite. Barium associated with biogenic opal is well known of these marginal basins of high biological productivity. Barium would be

mobilized by dissolution from biological detritus in sulfate-free pore waters and emitted by seep fluids. Such a mechanism had been suggested for barites at seeps along the Peru subduction and the Sakhalin transform fault (Torres et al. 1996; Aloisi et al. 2004b).

Tentatively though, two criteria may have emerged for transform fault seepage: (1) $^{87}Sr/^{86}Sr$ in fluids from the interaction with the underlying oceanic plate (Scholz et al. 2009) and (2) neo-formation of smectite recovered at depth from the sliding surfaces of the San Andrea Fault zone (Carpenter et al. 2011). Currently, it is difficult to envision that neo-formation of smectite may have any relevance to seeps, yet the sorely neglected studies of lithic material ejected from mud volcanoes may prove successful if the newly formed smectite in question may be differentiated from detrital smectite.

Some significant and speculative issues

Budgets of volatile emissions from seeps and retention of carbon as authigenic carbonates

Several approaches are in use to estimate the water output from the subducting sediment packages at convergent margins. One depends on porosity reduction and rate of subduction to yield water loss with distance from the deformation front (Saffer 2003; Moore et al. 2011). The other is based on measured and/or modeled emission rates at seep sites and up-scaling (Wallmann et al. 2006; Hensen et al. 2004; Ranero et al. 2008; Freundt et al. 2014; Karaca et al. 2012).

Restored structural sections that partition total shortening into fault slip and volume loss yield dewatering rates of ~10 $km^3\ Ma^{-1}$ per km of length as shown for the Nankai subduction zone (Moore et al. 2011); this approach appears attractive. However, according to the authors, it does not include the water loss from soft sediments during initial accretion, which might be the reason for discrepancies with seepage rates up-scaled from direct measurements. To improve this situation modeled flow rates from pore water profiles, bubble and fluid escape from seepage and the degree of biological methane oxidation (benthic filter) need to be better quantified. Deep-sea landers equipped with flux meters deployed at single sites (Tryon et al. 2001; Linke et al. 2005; Fürli et al. 2009) have recorded flow rates between $<10^{-3}$ and $>10^2$ cm $year^{-1}$. A geo-acoustic technique, GasQuant, based on the backscatter intensity of bubbles, horizontal scans of escaping plumes at the sea floor and integration of bubble spectra provides total gas fluxe estimates (Greinert 2008; Schneider von Deimling et al. 2011). These techniques combined with characterizing seep footprints should be refined and results compared to and harmonized with those from the geophysical approach.

Finally, if the biota at the seafloor and in the water column consume methane aerobically, the carbon is largely added as CO_2 to the seawater. If they consume methane anaerobically (AOM), the carbon is retained as authigenic carbonates (Treude 2012). Partitioning the methane-C sink from biological oxidation between seawater bicarbonate and mineral carbonate is a scientific challenge that has not been addressed as of today. The high apparent seafloor oxygen consumption and the apparently insufficient methane–carbon supply (Boetius and Wenzhöfer 2013) more than highlights the need for accurate budgeting.

Fossilization of microbial structures involved in AOM

Documentation of microbial activity from ancient seeps is progressing rapidly. The geologic time scale for seep activity is steadily being pushed back, with ancient plate boundaries and passive margins being recognized as characteristic settings (Campbell et al. 2002; Kiel 2009, 2010). Sediment fabric and organic geochemistry of geological material will continue to yield sites of ancient seeps. The concern over contamination of geological samples is not as serious as with recent material since microbial bodies are fully encased in the carbonate matrix that formed during AOM. Likewise, preparatory work in isolating biomarkers from authigenic carbonates ascertains contamination-free samples such as the miniaturized biosignature extraction procedures introduced recently (Leefmann et al. 2008).

Abundant structures of suspected fossilized microbes are present in seep carbonates. Among these are filamentous, rod-shaped, cylindrical, spindle- and dumbbell-shaped bodies and rice-shaped grains that await identification (Peckmann et al. 2004; Han et al. 2008; Crémiere et al. 2012). Fossilized bodies, resembling microbial morphologies and consisting wholly of AOM-carbonates, e.g., aragonite, high-Mg-calcite, and dolomite grains, and their biomarkers will provide considerable new knowledge. A breakthrough in this approach is that sulfate-reducing bacteria are able to directly form dolomite grains via a selective biofilm that actively alters the Mg/Ca ratio (Krause et al. 2012).

Elusive carbonates from serpentinization at subducting margins

If the return flow pathway of fluids released from serpentinization of the down-going oceanic plate is directly into bottom waters instead of through thick fore-arc sediments, such fluids may maintain high-pH values, Mg-, Ca-, and aqueous SiO_2-contents from dissolution of the ultramafic crustal minerals. Mixing at the slightly more acidic pH of seawater and with dissolved inorganic carbonate species (DIC) would result in carbonate mineral precipitation analogous to those chimneys formed from the products of serpentinized

oceanic crust at hydrothermal sites. The most likely site for emission of such fluids is at the trench-outer rise, usually quite deep (>4,000 m) such that carbonate formations might have escaped detection so far. Geophysical methods constrain the trench-outer rise offshore Nicaragua as a region underlain by serpentinized and highly fractured oceanic plate (Ivandic et al. 2010). A search there for subduction zone chimneys along with molecular hydrogen emissions would be a scientific objective for future convergent margin studies. Its relevance is seen in that the hypothetical carbonates could represent a hitherto unrecognized global CO_2-sink. This would complement estimates of CO_2 sequestered in onshore ophiolite massifs and ultramafic intrusions as well as offshore slow-spreading ridge segments and magmatic fore-arcs as currently debated (Kelemen et al. 2011).

Far-out option for reconstructing paleo-seawater from seep products

Pseudomorphs of carbonates after ikaite, an authigenic 6-hydrated calcium carbonate frequently found in the geologic record as well as in seep settings, has long been associated with polar environments (Whiticar and Suess 1998). This characterization does not strictly hold, as other environments of ikaite formation have been identified (Buchardt et al. 1997; Jansen et al. 1987), although generally a cold water environment seems to be favored (Schubert et al. 1997). Crude attempts to glean information on the temperature of formation from O-istotopes of ikaite, recovered from the Bransfield Strait and the Sea of Okhotsk (both at bottom water temperatures around freezing) yielded temperatures of -1 ± 1 °C (Suess et al. 1981; Greinert and Derkachev 2004). Thereby, the isotopic composition of the seawater from the Okhotsk Sea site was diluted by meteoric water, and more importantly, it remained unclear why calcium carbonate hexahydrate (ikaite) should behave like anhydrous calcite with regard to O-isotope fractionation. Experimental work on synthetic ikaites (Rickaby et al. 2006) showed that the crystal water of the hydrated carbonate phase preserves the original $\delta^{18}O$ of the precipitating water and the authors suggest its potential usefulness as proxy for ancient seawater. As $\delta^{18}O$(sw) is a crucial factor for calculating the temperature of formation from the O-isotopes, a search for hydrated authigenic carbonates among the seep products might yield surprising results. Ikaites are rarely preserved from seep sites; however, gas hydrates are ubiquitous. Much work has been done on hydrate water of methane hydrates, unfortunately—as of now—no clear relationship has emerged between the $\delta^{18}O$ of the precipitating fluid and the water retained in the clathrate structure (Maekawa 2004) that might be used as a proxy for ancient seawater.

Acknowledgments This article is a much expanded version of a review entitled: Marine cold seeps; Suess (2010) in: Handbook of Hydrocarbon and Lipid Microbiology, edited by Kenneth N. Timmis and published by Springer, Heidelberg. The editor and the publication staff of Springer graciously gave permission to build on this previously published material, including the use of several illustrations. Marc-André Gutscher (Brest), Gerhard Bohrmann (Bremen), Peter Linke and Tina Treude (both Kiel), Florian Scholz and Marta Torres (both Corvallis) provided advice and material, I thank them much for always responding promptly. I wish to thank Gerhard Bohrmann and Klaus Wallmann for thorough reviews that helped better focus this review on the geologic framework of marine cold seeps. I acknowledge the College of Earth, Ocean and Atmospheric Sciences, Oregon State University, Corvallis, for the Courtesy Appointment extended to me. Zona Suess helped, as always, with the intricacies of the English language and the organization of the references. This publication is Contribution No. 265 of the Sonderforschungsbereich 574 Volatiles and Fluids in Subduction Zones at Kiel University.

References

Aloisi G, Pierre C, Rouchy C, Foucher JP, Woodside J, The MEDINAUT Scientific Party (2000) Methane-related authigenic carbonates of eastern Mediterranean Sea mud volcanoes and their possible relation to gas hydrate destabilisation. Earth Planet Sci Lett 184:321–338

Aloisi G, Wallmann K, Drews M, Bohrmann G (2004a) Evidence for the submarine weathering of silicate minerals in Black Sea sediments: possible implications for the marine Li and B cycles. Geochem Geophys Geosyst 5:Q04007. doi:10.1029/2003GC000639

Aloisi G, Wallmann K, Bollwerk SM, Derkachev A, Bohrmann G, Suess E (2004b) The effect of dissolved barium on biogeochemical processes at cold seeps. Geochim Cosmochim Acta 68(8):1735–1748

Baco AR, Rowden AA, Levin LA, Smith CR, Bowden DA (2010) Initial characterization of cold seep faunal communities on the New Zealand Hikurangi margin. Mar Geol 272:251–259

Barnes PM, Lamarche G, Bialas J, Henrys S, Pecher I, Netzeband GL, Greinert J, Mountjoy JJ, Pedley K, Crutchley G (2010) Tectonic and geological framework for gas hydrates and cold seeps on the Hikurangi subduction margin, New Zealand. Mar Geol 272:26–48

Barrie JV, Conway KW, Harris PT (2013) The Queen Charlotte Fault, British Columbia: seafloor anatomy of a transform fault and its influence on sediment processes. Geo-Mar Lett 33:311–318

Bayon G, Pierre C, Etoubleau J, Voisset M, Cauquil E, Marsset T, Sultan N, Le Drezen E, Fouquet Y (2007) Sr/Ca and Mg/Ca ratios in Niger Delta sediments: implications for authigenic carbonate genesis in cold seep environments. Mar Geol 241:93–109

Bayon G, Birot D, Ruffine L, Caprais JC, Ponzevera E, Bollinger C, Donval JP, Charlou JL, Voisset M, Grimaud S (2011) Evidence for intense REE scavenging at cold seeps from the Niger Delta margin. Earh Planet Sci Lett 312(3–4):443–452

Birgel D, Himmler T, Freiwald A, Peckmann J (2008) A new constraint on the antiquity of anaerobic oxidation of methane: late Pennsylvanian seep limestones from southern Nambia. Geology 36:543–546

Boetius A, Wenzhöfer F (2013) Seafloor oxygen consumption fuelled by methane from cold seeps. Nat Geosci 6:725–734. doi:10.1038/NGEO1926

Boetius A, Ravenschlag K, Schubert CJ, Rickert D, Widdel F, Gieseke A, Amann R, Jørgensen BB, Witte U, Pfannkuche O (2000) A

marine consortium apparently mediating anaerobic oxidation of methane. Nature 407:623–626
Bohrmann G, Jørgensen BB (eds) (2010) Proceedings of the 9th international conference on gas in marine sediments, Bremen, Germany. Geo-Mar Lett SI 30(3/4):151–476
Bohrmann G, Greinert J, Suess E, Torres ME (1998) Authigenic carbonates from the Cascadia subduction zone and their relation to gas hydrate stability. Geology 26:647–650
Bohrmann G, Linke P, Suess E, Pfannkuche O (eds) (2000) RV SONNE Cruise Report SO143, TECFLUX-I GEOMAR Report 93, 217 pp
Bohrmann G, Ivanov MK et al (2003) Mud volcanoes and gas hydrates in the Black Sea: new data from Dvurechenskii and Odessa mud volcanoes. Geo-Mar Lett 23(3–4):239–249
Buchardt B, Seaman P, Stockmann G, Vous M, Wilken U, Duwel L, Kristiansen A, Jenner C, Whiticar MJ, Kristensen RM, Petersen GH, Thorbjorn L (1997) Submarine columns of ikaite tufa. Nature 390:129–130
Buerk D, Klaucke I, Sahling H, Weinrebe W (2010) Morpho-acoustic variability of cold seeps on the continental slope offshore Nicaragua: result of fluid flow interaction with sedimentary processes. Mar Geol 275:53–65
Burke WH, Denison RE, Hetherington EA, Koepnick RB, Nelson HF, Otto JB (1982) Variation of seawater $^{87}Sr/^{86}Sr$ throughout Phanerozoic time. Geology 10:516–519
Camerlenghi A, Cita MB, Della Vedova M, Fusi N, Mirabile LG, Pellis G (1995) Geophysical evidence for mud diapirism on the Mediterranean Ridge accretionary complex. Mar Geophys Res 17:115–141
Campbell KA (2006) Hydrocarbon seep and hydrothermal vent palaeo-environments: past developments and future research directions. Palaeogeogr Palaeoclimat Palaeoecol 232:362–407
Campbell KA, Farmer JD, DeMarais D (2002) Ancient hydrocarbon seeps from the Mesozoic convergent margin of California: carbonate geochemistry, fluids and paleoenvironment. Geofluids 2:63–94
Carpenter BM, Marone C, Saffer DM (2011) Weakness of the San Andreas Fault revealed by samples from the active fault zone. Nat Geosci 4:251–254
Chan LH, Kastner M (2000) Lithium isotope compositions of pore fluids and sediments in the Costa Rica subduction zone: implications for fluid processes and sediment contribution in the arc volcanoes. Earth Planet Sci Lett 183:275–290
Chen D, Huang Y, Yuan X, Cathles LM III (2005) Seep carbonates and preserved methane oxidizing bacteria and sulfur reducing bacteria fossils suggest recent gas venting an the seafloor in the northeastern South China. Mar Petrol Geol 22:613–621
Collett T et al (2008) Indian continental margin gas hydrate prospects: results of the Indian national gas hydrate program (NGHP) Exp. 01. In: Proceedings of the 6th International conference gas hydrates, Vancouver, BC, Canada July 6–10. https://circle.ubc.ca/handle/2429/1022
Colten-Bradley VA (1987) Role of pressure in smectite dehydration: effects on geopressure and smectite to illite transformation. Am Assoc Petrol Geol Bull 71:1414–1427
Cordes EE, Carney SL, Hourdez S, Carney R, Brooks JM, Fisher CR (2007) Cold seeps of the deep Gulf of Mexico: community structure and biogeographic comparisons to Atlantic and Caribbean seep communities. Deep Sea Res I 54:637–653
Crémiere A, Pierre C, Blanc-Valleron MM, Zitter T, Cagatay MN, Henry P (2012) Methane-derived authigenic carbonates along the North Anatolian fault system in the Sea of Marmara (Turkey). Deep Sea Res I 66:114–130
Crutchley GJ, Berndt C, Geiger S, Klaeschen D, Papenberg C, Klaucke I, Hornbach MJ, Bangs NLB, Maier C (2013) Drivers of focused fluid flow and methane seepage at south Hydrate Ridge, offshore Oregon, USA. Geology 41:551–554
Dählmann A, de Lange G (2003) Fluid–sediment interactions at eastern Mediterranean mud volcanoes: a stable isotope study from ODP Leg 160. Earth Planet Sci Lett 212:377–391
De Batist M, Khlystov O (eds) (2012) Proceedings of the 10th international conference on gas in marine sediments, Listvyanka, Russia. Geo-Mar Lett SI 32(5/6):373–562
Decarreau AN, Vigier N, Pálkováa H, Petita S, Vieillarda P, Fontainea C (2012) Partitioning of lithium between smectite and solution: an experimental approach. Geochim Cosmochim Acta 85:314–325
Dupré S, Woodside J, Foucher JP, de Lange G, Mascle J, Boetius A, Mastalerz V, Stadniskaia A, Ondréas H, Huguen C, Harmégnies F, Gontharet S, Loncke L, Deville HEN, Omoregie E, Roy KOL, Fiala-Medioni A, Dählmann A, Caprais JC, Prinzhofer A, Sibuet M, Pierre C, NAUTINIL Scientific Party (2007) Seafloor geological studies above active gas chimneys off Egypt (Central Nile Deep Sea Fan). Deep Sea Res 54:1146–1172
Elvert M, Suess E, Whiticar M (1999) Anaerobic methane oxidation associated with marine gas hydrates. Superlight C-isotopes from saturated and unsaturated C_{20} and C_{25} irregular isoprenoids. Naturwissenschaften 86:295–300
Feng D, Roberts HH, Cheng H, Peckmann J, Bohrmann G, Edwards RL, Chen D (2010) U/Th dating of cold-seep carbonates: an initial comparison. Deep Sea Res II 57:2055–2060
Feseker T, Foucher JP, Harmegnies F (2008) Fluid flow or mud eruptions? Sediment temperature distribution on Håkon Mosby mud volcano, SW Barents Sea slope. Mar Geol 247:194–207
Feseker T, Brown K, Blanchet C, Scholz F, Nuzzo M, Reitz A, Schmidt M, Hensen C (2010) Active mud volcanoes on the upper slope of the western Nile deep-sea fan—first results from the P362/2 cruise of R/V Poseidon. Geo-Mar Lett 30(3/4):169–186
Flueh ER, Suess E, Soeding E (eds) (2004) Cruise Report SO173/1 and SO173/3+4 subduction II. GEOMAR Report 115, 491
Foucher JP, Dupré S, Scalabrin C, Feseker T, Harmegnie F, Nouzé H (2010) Changes in seabed morphology, mud temperature and free gas venting at the Hakon Mosby mud volcano, offshore northern Norway, over the time period 2003–2006. Geo-Mar Lett 30(3–4):157–167
Freundt A, Grevemeyer I, Rabbel W et al (2014) Volatile (H2O, CO2, Cl, S) budget of the Central American subduction zone. Int J Earth Sci. doi:10.1007/s00531-014-1001-1
Freytag JK, Girguis PR, Bergquist DC, Andras JP, Childress JJ, Fisher CR (2001) A paradox resolved: sulfide acquisition by roots of seep tubeworms sustains net chemoautotrophy. Proc Natl Acad Sci 98:13408–13413
Fryer P, Mottl M, Johnson L, Haggerty L, Phipps S, Maekawa H (1995) Serpentine bodies in the forearc of Western Pacific convergent margins: origin and associated fluids. In: Taylor B, Natland J (eds) Active margins and marginal basins of the Western Pacific. Am Geophys Union Geophys Monogr 88:259–279
Fürli E, Hilton DR, Brown KM, Tryon MD (2009) Helium systematics of cold seep fluids at Monterey Bay, California, USA: temporal variations and mantle contributions. Geochem Geophys Geosyst 10(8):Q08013. doi:10.1029/2009GC002557
Gallardo AH, Marui A (2006) Submarine groundwater discharge: an outlook of recent advances and current knowledge. Geo-Mar Lett 26:102–113
Garcia-Gil S, Judd A (2007) Gas in marine sediments VIII: an introduction to the Vigo conference of the shallow gas group. Geo-Mar Lett 27:71–74
Ge L, Jiang SY, Swennen R et al (2010) Chemical environment of cold seep carbonate formation on the northern continental slope

of South China Sea: evidence from trace and rare earth element geochemistry. Mar Geol 277(1–4):21–30
Geersen J, Behrmann JH, Völker D, Krastel S, Ranero CR, Diaz-Naveas J, Weinrebe W (2011) Active tectonics of the South Chilean marine fore arc (35°S–40°S) Tectonics 30. doi:10.1029/2010TC002777
Geli L, Henry P, Zitter T, MARNAUT Scientific Party (2008) Gas emissions and active tectonics within the submerged section of the North Anatolian Fault zone in the Sea of Marmara. Earth Planet Sci Lett 274:34–39
German CR, Ramirez-Llodra E, Baker MC, Tyler PA, ChEss Scientific Steering Committee (2011) Deep-Water chemosynthetic ecosystem research during the census of marine life decade and beyond: a proposed deep-ocean road map. PLoS One 6(8):e23259
Gontharet S, Pierre C, Blanc-Valleron MM, Rouchy JM, Fouqet Y, Bayon G, Foucher JP, Woodside J, Mascle J et al (2007) Nature and origin of diagenetic carbonate crusts and concretions from mud volcanoes and pockmarks of the Nile deep-sea fan (eastern Mediterranean Sea). Deep Sea Res II 54:1292–1311
Gracia A, Rangel-Buitrago N, Sellanes J (2010) Evidences of the presence of Methane Seeps in the Colombian Caribbean Sea. EGU general assembly, Vienna, p 3632
Greinert J (2008) Monitoring temporal variability of bubble release at seeps: the hydroacoustic swath system GasQuant. J Geophys Res 113. doi:10.1029/2007JC004704
Greinert J, Derkachev A (2004) Glendonites and methane-derived Mg-calcites in the Sea of Okhotsk, eastern Siberia: implications of a venting-related ikaite/glendonite formation. Mar Geol 204:129–144
Greinert J, Bohrmann G, Suess E (2001) Gas hydrate-associated carbonates and methane venting at Hydrate Ridge: classification, distribution and origin of authigenic lithologies. In: Paull C, Dillon W (eds) Natural gas hydrates: occurrence, distribution, and detection. Am Geophys Union Wash Monogr 124:99–113
Greinert J, Bollwerk SM, Derkachev A, Bohrmann G, Suess E (2002) Massive barite deposits and carbonate mineralization in the Derugin Basin, Sea of Okhotsk: precipitation processes at cold seep sites. Earth Planet Sci Lett 203:165–180
Greinert J, Artemov Y, Egorov V, De Batist M, McGinnis D (2006) 1300-m-high rising bubbles from mud volcanoes at 2080 m in the Black Sea: hydroacoustic characteristics and temporal variability. Earth Planet Sci Lett 244:1–15
Greinert J, Bialas J, Lewis K, Suess E (eds) (2010) Methane seeps at the Hikurangi Margin, New Zealand. Mar Geol 272. doi:10.1016/j.margeo.2010.02.018
Gutscher MA, Dominguez S, Westbrook GK, Le Roy P, Rosas F, Duarte CD, Terrinha P, Miranda JM, Graindorge D, Gailler A, Sallares V, Bartolome R (2012) The Gibraltar subduction: a decade of new geophysical data. Tectonophysics 574(576):72–91
Haas A, Peckmann J, Elvert M, Sahling H, Bohrmann G (2010) Patterns of carbonate authigenesis at the Kouilou pockmarks on the Congo deep-sea fan. Mar Geol 268:129–136
Haeckel M, Suess E, Wallmann K, Rickert D (2004) Rising methane gas-bubbles form massive hydrate layers at the seafloor. Geochim Cosmochim Acta 68:4335–4345
Haeckel M, Boudreau BP, Wallmann K (2007) Bubble-induced porewater mixing: a 3-D model for deep porewater irrigation. Geochim Cosmochim Acta 71:5135–5154
Haffert L, Haeckel M, Liebetrau V, Berndt C, Hensen C, Nuzzo M, Reitz A, Scholz F, Schönfeld J, Perez-Garcia C, Weise SW (2013) Fluid evolution and authigenic mineral paragenesis related to salt diapirism—the Mercator mud volcano in the Gulf of Cadiz. Geochim Cosmochim Acta 106:261–286
Halliday EJ, Barrie JV, Chapman NR, Rohr KMM (2008) Structurally controlled hydrocarbon seeps on a glaciated continental margin, Hecate Strait, offshore British Columbia. Mar Geol 252:193–206
Han X, Suess E, Sahling H, Wallmann K (2004) Fluid venting activity on the Costa Rica margin: new results from authigenic carbonates. Int J Earth Sci 93:596–611
Han X, Suess E, Huang Y, Wu N, Bohrmann G, Su X, Eisenhauer A, Rehder G, Fang Y (2008) Jiulong methane reef: microbial mediation of seep carbonates in the South China Sea. Mar Geol 249:243–256
Han X, Suess E, Liebetrau V, Eisenhauer A, Huang YY (2014) Past methane release events and environmental conditions at the upper continental slope of the South China Sea: constraints from seep carbonates (this volume)
Heeschen KU, Haeckel M, Klaucke I, Ivanov MK, Bohrmann G (2011) Quantifying in situ gas hydrates at active seep sites in the eastern Black Sea using pressure coring technique. Biogeosciences 8:3555–3565
Hensen C, Wallmann K, Schmidt M, Ranero CR, Suess E (2004) Fluid expulsion related to mud extrusion off Costa Rica—a window to the subducting slab. Geology 32:201–204
Hensen C, Nuzzo M, Hornibrook E, Pinheiro LM, Bock B, Magalhaes VH, Brückmann W (2007) Sources of mud volcano fluids in the Gulf of Cadiz—indications for hydrothermal imprint. Geochim Cosmochim Acta 71:1232–1248
Hilario A, Cunha MR (2008) On some frenulate species (Annelida: Polychaeta: Siboglinidae) from mud volcanoes in the Gulf of Cadiz (NE Atlantic). Sci Mar 72(2):361–371
Himmler T, Bach W, Bohrmann G, Peckmann J (2010) Rare earth elements in authigenic methane-seep carbonates as tracers for fluid composition during early diagenesis. Chem Geol 277:126–136
Himmler T, Haley BA, Torres ME, Klinkhammer GP, Bohrmann G, Peckmann J (2013) Rare earth element geochemistry in cold seep pore waters of Hydrate Ridge, northeast Pacific Ocean. Geo-Mar Lett 33:369–379
Hinrichs KU, Hayes JM, Sylva SPO, Brewer PG, DeLong EF (1999) Methane-consuming archaebacteria in marine sediments. Nature 398:802–805
Hovland M (2007) Discovery of prolific natural methane seeps at Gullfaks, northern North Sea. Geo-Mar Lett 27:197–201
Huang C-Y, Chien C-W, Zhao M-X, Li H-C, Iizuka Y (2006) Geological study of active cold seeps in the syn-collision accretionary prism Kaoping slope off SW Taiwan. Terr Atmos Ocean Sci 17(4):679–702
Iglesias J, Ercilla G, García-Gil S, Judd AG (2010) Pockforms: an evaluation of pockmark-like seabed features on the Landes Plateau, Bay of Biscay. Geo-Mar Lett 30:207–219
IODP Prelim. Rept. Expedition 344 Scientists (2013) Costa Rica Seismogenesis project, Program A Stage 2 (CRISP-A2): sampling and quantifying lithologic inputs and fluid inputs and outputs of the seismogenic zone. Prel Rep 344. doi:10.2204/iodp.pr.344
Ivandic M, Grevemeyer I, Bialas J, Petersen CP (2010) Serpentinization in the trench-outer rise region offshore of Nicaragua: constraints from seismic refraction and wide-angle data. Geophys J Int 180:1253–1264
Ivanov AV (1963) Pogonophora. Publ Consultants Bureau, New York
Jansen JHF, Woensdregt CF, Kooistra MJ, van de Gaast SJ (1987) Ikaite pseudomorphs in the Zaire deep-sea fan: an intermediate between calcite and porous calcite. Geology 15:245–248
Jarrard RD (2003) Subduction fluxes of water, carbon dioxide, chlorine, and potassium. Geochem Geophys Geosyst 4(5):8905. doi:10.1029/2002GC000392
Jeong KS, Cho JH, Kim SR, Hyun S, Tsunogai U (2004) Geophysical and geochemical observations on actively seeping hydrocarbon gases on the south-eastern Yellow Sea continental shelf. Geo-Mar Lett 24:53–62

Jones AT, Greinert J, Bowden DA, Klaucke I, Petersen CJ, Netzeband GL, Weinrebe W (2010) Acoustic and visual characterization of methane-rich seabed seeps at Omakere Ridge on the Hikurangi Margin, New Zealand. Mar Geol 272:154–169

Judd AG, Hovland M (2007) Submarine fluid flow, the impact on geology, biology, and the marine environment. Cambridge University Press, Cambridge

Judd AG, Croker P, Tizzard L (2007) Extensive methane-derived authigenic carbonates in the Irish Sea. Geo-Mar Lett 27:259–267

Karaca D, Schleicher T, Hensen C, Linke P, Wallmann K (2012) Quantification of methane emission from bacterial mat sites at Quepos slide offshore Costa Rica. Int J Earth Sci. doi:10.1007/s00531-012-0839-3

Karpen V, Thomsen L, Suess E (2004) A new 'schlieren' technique application for fluid flow visualization at cold seep sites. Mar Geol 204:145–159

Kasten S, Nöthen K, Hensen C, Spieß V, Blumenberg M, Schneider RR (2012) Gas hydrate decomposition recorded by authigenic barite at pockmark sites of the northern Congo Fan. Geo-Mar Lett. doi:10.1007/s00367-012-0288-9

Kelemen PB, Matter J, Streit EE, Rudge JF, Curry WB, Blusztajn J (2011) Rates and mechanisms of mineral carbonation in peridotite: natural processes and recipes for enhanced, in situ CO2 capture and storage. Annu Rev Earth Planet Sci 39:545–576

Kennicutt MC et al (1985) Vent-type taxa in a hydrocarbon seep region on the Louisiana slope. Nature 317:351–353

Kiel S (2009) Global hydrocarbon seep-carbonate precipitation correlates with deep-water temperatures and eustatic sea-level fluctuations since the Late Jurrasic. Terra Nova 21:279–284

Kiel S (ed) (2010) The Vent and Seep Biota: aspects from microbiology to ecosystems, vol, 33. Topics in geobiology. Springer, Heidelberg

Klaucke I, Weinrebe W, Petersen CJ, Bowden D (2010) Temporal variability of gas seeps offshore New Zealand: multi-frequency geoacoustic imaging of the Wairarapa area, Hikurangi margin. Mar Geol 272:49–58

Klaucke I, Weinrebe W, Linke P, Klaeschen D, Bialas J (2012) Sidescan sonar imagery of widespread fossil and active cold seeps along the central Chilean continental margin. Geo-Mar Lett 32:489–499

Knittel K, Boetius A, Lemke A, Eilers H, Lochte K, Pfannkuche O, Linke P (2003) Activity, distribution, and diversity of sulfate reducers and other bacteria in sediments above gas hydrate (Cascadia margin, Oregon). Geomicrobiol J 20:269–294. doi:10.1080/01490450390241008

Koleshnikov A, Kutcherov VG, Goncharov AF (2009) Methane-derived hydrocarbons produced under upper-mantle conditions. Nat Geosci 2:566–570

Krause S, Liebetrau V, Gorb S, Sanchez-Roman M, McKenzie JA, Treude T (2012) Microbial nucleation of Mg-rich dolomite in exopolymeric substances under anoxic modern seawater salinity: new insight into an old enigma. Geology 40(7):587–590

Krylova EM, Sahling H (2010) Vesicomyidae (Bivalvia): current taxonomy and distribution. PLoS One 5(4):e9957

Kulm LD, Suess E, Moore JC, Carson B, Lewis BT, Ritger SD, Kadko DC, Thornburg TM, Embley RW, Rugh WD, Massoth GJ, Langseth MG, Cochrane GR, Scamman RL (1986) Oregon subduction zone: venting, fauna, and carbonates. Science 231:561–566

Kutterolf S, Liebetrau V, Mörz T, Freundt A, Hammerich T, Garbe-Schönberg CD (2008) Lifetime and cyclicity of fluid venting at forearc mound structures determined by tephrostratigraphy and radiometric dating of authigenic carbonates. Geology 36(9):707–710

Leefmann T, Bauermeister J, Kronz A, Liebetrau J, Reitner J, Thiel V (2008) Miniturized biosignature analysis reveals implications for the formation of cold seep carbonates at Hydrate Ridge (off Oregon USA). Biogeosciences 5:731–738

León R, Somoza L, Medialdea T et al (2012) New discoveries of mud volcanoes on the Moroccan Atlantic continental margin (Gulf of Cádiz): morpho-structural characterization. Geo-Mar Lett 32:473–488

LePichon X, Ilyami T, Boulegue J, Charvet J et al (1987) Nankai trough and Zenisu ridge: a deep-sea submersible survey. Earth Planet Sci Lett 83(181):285–299

Levin LA (2005) Ecology of cold seep ecosystems: interactions of fauna with flow, chemistry and microbes. Oceanogr Mar Biol Annu Rev 43:1–46

Liebetrau V, Eisenhauer A, Linke P (2010) Cold seep carbonates and associated cold-water corals at the Hikurangi Margin, New Zealand: new insights into fluid pathways, growth structures and geochronology. Mar Geol 272:307–318

Liebetrau V, Augustin N, Kutterolf S, Schmidt M, Eisenhauer A, Garbe-Schönberg D, Weinrebe W (2014) Cold seep driven carbonate deposits at the Central American Forearc—contrasting evolution and timing in escarpment and mound settings. Int J Earth Sci (this volume)

Limonov AF, Woodside JM, Cita MB, Ivanov MK (1996) The Mediterranean Ridge and related mud diapirism: a background. Mar Geol 132:7–19

Lin AT, Liu C-S, Lin C–C, Schnurle P, Chen G-Y, Liao W-Z, Teng L-S, Chuang H-J, Wu M-S (2008) Tectonic features associated with the overriding of an accretionary wedge on top of a rifted continental margin: an example from Taiwan. Mar Geol 255:186–203

Linke P (ed) (2011) FS SONNE Fahrtbericht/Cruise Report SO-210 ChiFlux. IFM-GEOMAR Report, pp 112, ISSN Nr. 1614-6298

Linke P, Wallmann K, Suess E, Hensen C, Rehder G (2005) In situ benthic fluxes from an intermittently active mud volcano at the Costa Rica convergent margin. Earth Planet Sci Lett 235:79–95

Loncke L, Mascle J, Fanil Scientific Party (2004) Mud volcanoes, gas chimneys, pockmarks and mounds in the Nile deep-sea fan (Eastern Mediterranean): geophysical evidences. Mar Pet Geol 21:669–689

Loncke L, Gaullier V, Mascle J, Vendeville B, Camera L (2006) The Nile deep-sea fan: an example of interacting sedimentation, salt tectonics, and inherited subsalt paleotopographic features. Mar Pet Geol 23:297–315

Lonsdale P (1979) A deep-sea hydrothermal site on a strike-slip fault. Nature 281:531–534

Lu H-F, Liu J, Chen F, Liao Z-L, Sun X-M, Su X (2005) Mineralogy and stable isotope composition of authigenic carbonates in bottom sediments in the offshore area of southwest Taiwan, South China Sea, evidence for gas hydrate occurrence. Earth Sci Fronties 12(3):268–276

Ludwig KA, Kelley DS, Butterfield DA, Nelson BK, Früh-Green G (2006) Formation and evolution of carbonate chimneys at the Lost City hydrothermal field. Geochim Cosmochim Acta 70:3625–3645

MacDonald IR, Reilly JF, Guinasso NL Jr, Brooks JM, Carney RS, Bryant WA, Bright TJ (1990) Chemosynthetic mussels at a brine-filled pockmark in the northern Gulf of Mexico. Science 248:1096–1099

MacDonald IR et al (2004) Asphalt volcanism and chemosynthetic life in the Campeche Knolls, Gulf of Mexico. Science 304:999–1002

Maekawa T (2004) Experimental study on isotopic fractionation in water during gas hydrate formation. Geochem J 38:129–138

Martin RA, Nesbitt EA, Campbell KA (2010) The effects of anaerobic methane oxidation on benthic foraminiferal assemblages and stable isotopes on the Hikurangi Margin of eastern New Zealand. Mar Geol 272:270–284

Mastarlerz V, de Lange GJ, Dählmann A, Feseker T (2007) Active venting at the Isis mud volcano, offshore Egypt: origin and migration of hydrocarbons. Chem Geol 246:87–106

Matsumoto R (1989) Isotopically heavy oxygen-containing siderite derived from the decomposition of methane hydrate. Geology 17:707–711

Matsumoto R, Borowski WS (2000) Gas hydrate estimates from newly determined oxygen isotopic fractination a_{GH-IW} and $\delta^{18}O$ anomalies of the interstitial waters: Leg 164, Blake Ridge. In: Paull CK, Matsumoto R, Wallace PJ, Dillon WP (eds) Proc ODP Sci Res 164:59–66

Matsumoto R, Riedel M, Lin S, Ryu BJ, Sain K, Lu H (eds) (2011) Occurrence and exploration of gas hydrate in the marginal seas and continental margin of the Asia, India and Oceania region. Mar Pet Geol 28(10):1751–1986

Mau S, Rehder G, Sahling H, Schleicher T, Linke P (2012) Seepage of methane at Jaco Scar, a slide caused by seamount subduction offshore Costa Rica. Int J Earth Sci. doi:10.1007/s00531-012-0822-z

Mavromatis V, Botz R, Schmidt M, Liebetrau V, Hensen C (2012) Formation of carbonate concretions in surface sediments of two mud mounds offshore Costa Rica: a stable isotope study. Int J Earth Sci. doi:10.1007/s00531-012-0843-7

Mazzini A, Ivanov MK, Nermoen A, Bahr A, Bohrmann G, Svensen H, Planke S (2008) Complex plumbing systems in the near subsurface: geometries of authigenic carbonates from Dolgovskoy Mound (Black Sea) constrained by analogue experiments. Mar Pet Geol 25:457–472

McQuay EL, Torres ME, Collier RW, Huh C, McManus J (2008) Contribution of cold seep barite to the barium geochemical budget of a marginal basin. Deep Sea Res 55:801–811

Milucka J, Ferdelman TG, Polerecky L, Franzke D, Wegener G, Schmid M, Lieberwirth I, Wagner M, Widdel F, Kuypers MMM (2012) Zero-valent sulphur is a key intermediate in marine methane oxidation. Nature 491:541–546

Moore CJ (1999) Seeps give a peek into plumbing. Am Assoc Pet Geol Expl 99:22–23

Moore GF, Bangs NL, Taira A, Kuramoto S, Pangborn E, Tobin HJ (2007) Three-dimensional splay fault geometry and implications for tsunami generation. Science 318:1128–1131

Moore GF, Saffer D, Studer M, Costa Pisani P (2011) Structural restoration of thrusts at the toe of the Nankai Trough accretionary prism off Shikoku Island, Japan: implications for dewatering processes. Geochem Geophys Geosyst 12:Q0AD12. doi:10.1029/2010GC003453

Mottl MJ, Komor SC, Fryer P, Moyer CL (2003) Deep-slab fluids fuel extremophilic Archaea on a Mariana forearc serpentinite mud volcano: Ocean Drilling Program Leg 195. Geochem Geophys Geosyst 4:9009. doi:10.1029/2003GC000588

Mottl MJ, Wheat CG, Fryer P, Gharib J, Martin JB (2004) Chemistry of springs across the Mariana forearc shows progressive devolatilization of the subducting plate. Geochim Cosmochim Acta 68:4915–4933

Naudts L, Greinert J, Artemov Y, Staelens P, Poort J, Van Rensbergen P, De Batist M (2006) Geological and morphological setting of 2778 methane seeps in the Dnepr paleo-delta, northwestern Black Sea. Mar Geol 227:177–199

Niemann H, Fischer D, Graffe D, Knittel K, Montiel A, Heilmayer O, Nöthen K, Pape T, Kasten S, Bohrmann G, Boetius A, Gutt J (2009) Biogeochemistry of a low-activity cold seep in the Larsen B area, western Weddell Sea, Antarctica. Biogeosciences 6:2383–2395

Niemann H, Linke P, Knittel K, MacPherson E, Boetius A, Brückmann W, Larvik G, Wallmann K, Schacht U, Omoregie E, Hiltons D, Brown K, Rehder G (2013) Methane-carbon flow into the benthic food web at cold seeps—a case study from the Costa Rica subduction zone. PLoS One 8(10):e74894

Nyman SL, Nelson CS, Campbell KA (2010) Miocene tubular concretions in East Coast Basin, New Zealand: analogue for the subsurface plumbing of cold seeps. Mar Geol 272:319

Olu-Le Roy K, Sibuet M, Fiala-Médioni A, Gofas S, Salas C, Mariotti A, Foucher JP, Woodside J (2004) Cold seep communities in the deep eastern Mediterranean Sea: composition, symbiosis and spatial distribution on mud volcanoes. Deep Sea Res I 51:1915–1936

Olu-Le Roy K, Caprais J, Fifis A, Fabri M, Galeron J, Budzinsky H, Le Menach K, Khripounoff A, Ondreas H, Sibuet M (2007) Cold-seep assemblages on a giant pockmark off West Africa: spatial patterns and environmental control. Mar Ecol 28:115–130

Orphan VJ, House CH, Hinrichs KU, McKeegan KD, DeLong EF (2001) Methane-consuming archaea revealed by directly coupled isotopic and phylogenetic analysis. Science 293:484–487

Palandri JL, Reed MD (2004) Geochemical models of metasomatism in ultramafic systems: serpentinization, rodingitization, and sea floor carbonate chimney precipitation. Geochim Cosmochim Acta 68(5):1115–1133

Pancost RD, Sinninghe Damsté JS, de Lint S, van der Maarel MJEC, Gottschal JC, The Medinaut Shipboard Scientific Party (2000) Biomarker evidence for widespread anaerobic methane oxidation in Mediterranean sediments by a consortium of methanogenic Archaea and Bacteria. Appl Environ Microbiol 66(3):1126–1132

Pape T, Kasten S, Zabel M, Bahr A, Abegg F, Hohnberg H-J, Bohrmann G (2010) Gas hydrates in shallow deposits of the Amsterdam mud volcano, Anaximander Mountains, northeastern Mediterranean Sea. Geo-Mar Lett 30:187–206

Pape T, Bahr A, Klapp SA, Abegg F, Bohrmann G (2011) High-intensity gas seepage causes rafting of shallow gas hydrates in the southeastern Black Sea. Earth Planet Sci Lett 307:35–46

Paull CK, Becker B, Commeau R, Freeman-Lynde RP, Neumann C, Corso WP, Golubic S, Hook JE, Sikes E, Curry J (1984) Biological communities at the Florida Escarpment resemble hydrothermal vent taxa. Science 226:965–967

Peacock SM (2001) Are the lower planes of double seismic zones caused by serpentine dehydration in subducting oceanic mantle? Geology 29:299–302

Peckmann J, Reimer A, Luth U, Luth C, Hansen BT, Heinicke C, Hoefs J, Reitner J (2001) Methane-derived carbonates and authigenic pyrite from the northwestern Black Sea. Mar Geol 177:129–150

Peckmann J, Thiel V, Reitner J, Taviani M, Aharon P, Michaelis W (2004) A microbial mat of a large sulfur bacterium preserved in a Miocene methane-seep limestone. Geomicrobiol J 21:247–255

Perez-Garcia C, Feseker T, Mienert J, Berndt C (2009) The Håkon Mosby mud volcano: 330000 years of focused fluid flow activity at the SW Barents Sea slope. Mar Geol 262(1/4):105–115

Peterson RN, Burnett WC, Taniguchi M, Chen J, Santos IR, Ishitobi T (2008) Radon and radium isotope assessment of submarine groundwater discharge in the Yellow River delta, China. J Geophys Res 113. doi:10.1029/2008JC004776

Pierre C, Fouquet Y (2007) Authigenic carbonates from methane seeps of the Congo deep-sea fan. Geo-Mar Lett 27(2/4):249–257

Pierre C, Mascle J, Imbert P (eds) (2014) Contributions from the 11th international conference on gas in marine sediments, Nice 2011. Geo-Mar Lett 34(2/3) (in press)

Prokurowski G et al (2008) Abiogenic hydrocarbon production at Lost City hydrothermal field. Science 319:604–607

Ranero CR, von Huene R (2000) Subduction erosion along the Middle America convergent margin. Nature 404:748–752

Ranero CR, Phipps Morgan J, McIntosh K, Reichert C (2003) Bending, faulting, and mantle serpentinization at the Middle America Trench. Nature 425:367–373

Ranero CR, Grevemeyer I, Sahling H, Barckhausen U, Hensen C, Wallmann K, Weinrebe W, Vannucchi P, von Huene R, McIntosh K (2008) Hydrogeological system of erosional convergent margins and its influence on tectonics and interplate seismogenesis. Geochem Geophy Geosys 9(3). doi:10.1029/2007GC001679

Rickaby REM, Shaw S, Bennitt G, Kennedy H, Zabel M, Lennie A (2006) Potential of ikaite to record the evolution of oceanic $\delta^{18}O$. Geology 34:497–500

Roberts HH, Boland BS (eds) (2010) Topial studies in oceanography: golf of Mexico Cold seeps. Deep Sea Res 57(21/23):1835–2060

Rongemaille E, Bayon G, Pierre C, Bollinger C, Chu NC, Fouquet Y, Riboulot V, Voisset M (2011) Rare earth elements in cold seep carbonates from the Niger delta. Chem Geol 286:196–206

Rossel PE, Lipp JS, Fredricks HF, Arnds J, Boetius A, Elvert M, Henrichs KU (2008) Intact polar lipids of anaerobic methanotrophic archaea and associated bacteria. Org Geochem 39:992–999

Rossel PE, Elvert M, Ramette A, Boetius A, Hinrichs K-U (2011) Factors controlling the distribution of anaerobic methanotrophic communities in marine environments: evidence from intact polar membrane lipids. Geochim Cosmochim Acta 75:164–184

Rüpke LH, Phipps-Morgan J, Hort M, Connolly JAD (2004) Serpentine and the subduction zone water cycle. Earth Planet Sci Lett 223:17–34

Saffer DM (2003) Pore pressure development and progressive dewatering in underthrust sediments at the Costa Rican subduction margin: comparison with Northern Barbados and Nankai. J Geophys Res 108:B5. doi:10.1029/202JB001787

Saffer DM, McKiernan AW (2009) Evaluation of in situ smectite dehydration as a pore water freshening mechanism in the Nankai Trough, offshore southwest Japan. Geochim Geophys Geosys 10(2). doi:10.1029/2008GC002226

Sahling H, Rickert D, Lee RW, Linke P, Suess E (2002) Macrofaunal community structure and sulfide flux at gas hydrate deposits from the Cascadia convergent margin; NE Pacific. Mar Ecol Prog Ser 231:121–138

Sahling H, Galkin SV, Salyuk A, Greinert J, Foerstel H, Piepenburg D, Suess E (2003) Depth-related structure and ecological significance of cold-seep communities. A case study from the Sea of Okhotsk. Deep Sea Res 50:1391–1409

Sahling H, Masson DG, Ranero CR, Hühnerbach V, Weinrebe W, Klaucke I, Bürk D, Brückmann W, Suess E (2008) Fluid seepage at the continental margin offshore Costa Rica and southern Nicaragua. Geochem Geophy Geosys 9(5). doi:10.1029/2008GC001978

Sassen R, Roberts HH, Carney R, Milkov A, DeFreitas DA, Lanoil B, Zhang CL (2004) Free hydrocarbon gas, gas hydrate and authigenic minerals in chemosynthetic communities of the northern Gulf of Mexico continental slope: relation to microbial process. Chem Geol 205:195–217

Schneider von Deimling J, Rehder G, Greinert J, McGinnnis DF, Boetius A, Linke P (2011) Quantification of seep-related methane gas emissions at Tommeliten, North Sea. Cont Shelf Res 31:867–878

Schnürle P, Liu C-S, Lin A-T, Lin S (2011) Structural controls on the formation of BSR over a diapiric anticline from a dense MCS survey offshore southwestern Taiwan. Mar Petrol Geol 28(10):1932–1942

Scholl DV, von Huene R (2007) Crustal recycling at modern subduction zones applied to the past—issues of growth and preservation of continental basement crust, mantle geochemistry, and supercontinent reconstruction. Geol Soc Am Mem 200:9–32

Scholz F, Hensen C, Reitz A, Romer RL, Liebetrau V, Meixner A, Weise SM, Haeckel M (2009) Isotopic evidence ($^{87}Sr/^{86}Sr$, $\delta^{7}Li$) for alteration of the oceanic crust at deep-rooted mud volcanoes in the Gulf of Cadiz, NE Atlantic Ocean. Geochim Cosmochim Acta 73:5444–5459

Scholz F, Hensen C, de Lange GJ, Haeckel M, Liebetrau V, Meixner A, Reitz A, Romer RL (2010) Lithium isotope geochemistry of marine pore waters—insights from cold seep fluids. Geochim Cosmochim Acta 74:3457–3459

Scholz F, Hensen C, Schmidt M, Geersen J (2013) Submarine weathering of silicate minerals and the extent of pore water freshening at active continental margins. Geochim Cosmochim Acta 100:200–216

Schubert CJ, Nürnberg D, Scheele N, Pauer F, Kriews M (1997) ^{13}C depletion in ikaite crystals: evidence for methane release from the Siberian shelves? Geo-Mar Lett 17:169–175

Sellanes J, Quiroga E, Neira C (2008) Megafauna community structure and trophic relationships at the recently discovered Concepcion Methane Seep Area, Chile ~36°S. ICES J Mar Sci Adv. doi:10.1093/icesjms/fsn099

Shakirov R, Obzhirov A, Suess E, Salyuk A, Biebow N (2004) Mud volcanoes and gas vents in the Okhotsk Sea area. Geo-Mar Lett 24:140

Sibuet M, Olu K (1998) Biogeography, biodiversity and fluid dependence of deep-sea cold-seep communities at active and passive margins. Deep Sea Res Part II 45:517–567

Soeding E, Wallmann K, Suess E, Flueh ER (eds) (2003) Cruise Report M54/2+3: Fluids and subduction Costa Rica 2002. GEOMAR Report 111; 336 pp

Sommer S, Linke P, Pfannkuche O, Schleicher T, Schneider von Deimling J, Reitz A, Haeckel M, Flögel S, Hensen C (2009) Seabed methane emissions and the habitat of frenulate tubeworms on the Captain Arutyunov mud volcano (Gulf of Cadiz). Mar Ecol Prog Ser 382:69–86

Suess E (ed) (2005) RV SONNE 177; South China Sea continental margin: geological methane budget and environmental effects of methane emissions and gas hydrates. IFM-GEOMAR Report 04. doi:10.3289/ifm-geomar_rep_4_2005

Suess E (2010) Marine cold seeps. In: Timmis KN (ed) Handbook of hydrocarbon and lipid microbiology, vol. 1, part 3. Springer, Heidelberg, pp 187–203. doi:10.1007/978-3-540-77587-4_12

Suess E, Linke P (2006) Der Ozean unter dem Meeresboden—Kalte Quellen als Oasen der Tiefsee. In: Wefer G (ed) Expedition Erde, 2nd edn, pp 88–101

Suess E, Balzer W, Hesse KF, Müller PJ, Ungerer CA, Wefer G (1981) CaCO3-hexahydrate from organic-rich sediments of the Antarctic shelf: precursors of glendonites. Science 216:1128–1131

Suess E, Carson B, Ritger SD, Moore JC, Jones ML, Kulm LD, Cochrane GR (1985) Biological communities at vent sites along the subduction zone off Oregon. Biol Soc Wash Bull 6:475–484

Teichert BMA, Eisenhauer A, Bohrmann G, Haase-Schramm A, Bock B, Linke P (2003) U/Th systematics and ages of authigenic carbonates from Hydrate Ridge, Cascadia Margin: recorders of fluid flow variations. Geochim Cosmochim Acta 67(20):3845–3857

Teichert BMA, Bohrmann G, Suess E (2005) Chemoherms on Hydrate Ridge—unique microbially-mediated carbonate buildups growing into the water column. Palaeogeogr Palaeoclimatol Palaeoecol 227:67–85

Tinivella U, Lodolo E (2000) The Blake Ridge bottom-simulating reflector transect: tomographic velocity field and theoretical model to estimate methane hydrate quantities. In: Paull CK, Matsumoto R, Wallace PJ, Dillon WP (eds) Proc ODP Sci Results 164:273–281. doi:10.2973/odp.proc.sr.164.237.2000

Tong H, Feng D, Cheng H et al (2013) Authigenic carbonates from seeps on the northern continental slope of the South China Sea:

new insights into fluid sources and geochronology. Mar Pet Geol 43:260–271

Torres ME, Bohrmann G, Suess E (1996) Authigenic barites and fluxes of barium associated with fluid seeps in the Peru subduction zone. Earth Planet Sci Lett 144:469–481

Torres ME, McManus J, Huh C-A (2002) Fluid seepage along the San Clemente Fault scarp: basin-wide impact on barium cycling. Earth Planet Sci Lett 203:181–194

Torres ME, Mix AC, Kinports K, Haley B, Klinkhammer G, McManus J, DeAngelis MA (2003) Is methane venting at the seafloor recorded by δ13C of benthic foraminifera shells? Paleoceanography 18(3). doi:10.1029/2002PA000824

Torres ME, Teichert BMA, Trehu AM, Borowski W, Tomaru H (2004) Relationship of pore water freshening to accretionary processes in the Cascadia margin: fluid sources and gas hydrate abundance. Geophys Res Lett 31:L22305. doi:10.1029/2004GL021219

Torres ME, Embley RW, Merle SG, Tréhu AM, Collier RW, Suess E, Heeschen KU (2009) Methane sources feeding cold seeps on the shelf and upper continental slope off central Oregon, USA. Geochem Geophys Geosys 10(11):Q11003. doi:10.1029/2009GC002518

Treude T (2012) Biogeochemical reactions in marine sediments underlying anoxic water bodies. In: Altenbach AV, Bernhard JM, Seckbach J (eds) Anoxia: evidence for Eucaryote survival and paleontological strategies. Series: cellular origin, life in extreme habitats and astrobiology 21:17–38

Treude T, Orphan V, Knittel K et al (2007) Consumption of methane and CO2 by methanotrophic microbial mats from gas seeps of the anoxic Black Sea. Appl Environ Microbiol 73:2271–2283

Tryon MD, Brown K, Dorman L, Sauter E (2001) A new benthic aqueous flux meter for very low to moderate discharge rates. Deep Sea Res I 48(9):2121–2146

Tryon MD, Henry P, Cagatay MN, Zitter TAC, Geli L, Gasperini L, Burnard P, Bourlange S, Grall C (2010) Pore fluid chemistry of the North Anatolian Fault Zone in the Sea of Marmara: a diversity of sources and processes. Geochem Geophys Geosys 11:1–22

van Avendonk HJA, Holbrook WS, Lizarralde D, Denyer P (2011) Structure and serpentinization of the subducting Cocos plate offshore Nicaragua and Costa Rica. Geochem Geophys Geosys 12(6). doi:10.1029/2011GC003592

van der Straaten F, Halama R, John T, Schenk V, Hauff F, Andersen N (2012) Tracing the effects of high-pressure metasomatic fluids and seawater alteration in blueschist-facies overprinted eclogites: implications for subduction channel processes. Chem Geol 292–293(2012):69–87

Vannucchi P, Fisher DM, Bier S, Gardner TW (2006) From seamount accretion to tectonic erosion: formation of Osa mélange and the effects of Cocos Ridge subduction in southern Costa Rica. Tectonics 25(4):TC2004. doi:10.1029/2005TC001855

Wallmann K (2001) The geological water cycle and the evolution of marine δ180 values. Geochim Cosmochim Acta 65:2469–2485

Wallmann K, Drews M, Aloisi G, Bohrmann G (2006) Methane discharge into the Black Sea and the global ocean via fluid flow through submarine mud volcanoes. Earth Planet Sci Lett 205:181–194

Wallmann K, Aloisi G, Haeckel M, Tishchenko P, Pavlova G, Greinert J, Kutterolf S, Eisenhauer A (2008) Silicate weathering in anoxic marine sediments. Geochim Cosmochim Acta 72:2895–2918

Wannamaker TG, Caldwell GR, Jiracek V, Maris GJ, Hill Y, Ogawa H, Bibby M, Bennie L, Heise W (2009) Fluid and deformation regime of an advancing subduction system at Marlborough, New Zealand. Nature 460:733–736

Warén A, Bouchet P (2009) New gastropods from deep-sea hydrocarbon seeps off West Africa. Deep Sea Res II 56:2326–2349

Watanabe Y, Nakai S, Hiruta A, Matsumoto R, Yoshida K (2008) U-Th dating of carbonate nodules from methane seeps off Joetsu, Eastern Margin of Japan Sea. Earth Planet Sci Lett 272(1–2):89–96

Weinrebe W, Flüh ER (eds) (2002) FS/RV SONNE Cruise Report SO163 SUBDUCTION I; GEOMAR Report 106, 531 pp

Westbrook GK, MEDRIFF Consortium (1995) Three brine lakes discovered in the seafloor of the Eastern Mediterranean. EOS Trans Am Geophys Union 76:313–318

Westbrook GH, Reston TJ (2002) The accretionary complex of the Mediterranean Ridge: tectonics, fluid flow and the formation of brine lakes—an introduction. Mar Geol 186:1–8

Whiticar MJ (1999) Carbon and hydrogen isotope systematics of bacterial formation and oxidation of methane. Chem Geol 161:291–314

Whiticar MJ, Suess E (1998) The cold carbonate connection between Mono Lake, California and the Bransfield Strait, Antarctica. Aquatic Geochem 4:429–454

Worzewski T, Jegen M, Kopp H, Brasse H, Taylor WT (2010) Magnetotelluric image of the fluid cycle in the Costa Rican subduction zone. Nat Geosci 4:108–111

Yang JY, Chung K-H, Jin Y-K, Shin K-H (2011) Characterizing lipid biomarkers in methanotrophic communities of gas hydrate-bearing sediments in the Sea of Okhotsk. Mar Pet Geol 28(10):1884–1898

Zapata-Hernandez G, Sellanes X, Thurber AR, Levin L A, Chazalon F, Linke P (2013) New insights on the trophic ecology of bathyal communities from the methane seep area of Concepcion, Chile (~36° S). Mar Ecol 35:1–21. doi:10.1111/maec.12-51

Zhang CL, Lanoil B (eds) (2004) Geomicrobiology and biogeochemistry of gas hydrates and hydrocarbon seeps. Chem Geol 205(3/4):387–486

Zitter TAC, Henry P, Aloisi G, Delaygue G, Cagatay MN, Mercier de Lepinay B, Al-Samir M, Fornacciari F, Tesmer M, Pekdeger A, Wallmann K, Lericolais G (2008) Cold seeps along the main Marmara Fault in the Sea of Marmara (Turkey). Deep Sea Res I 55:552–570